EGE UNIVERSITY GRADUATE SCHOOL OF APPLIED AND NATURAL SCIENCES

(MASTER OF SCIENCE THESIS)

ADSORPTION AND DESORPTION BEHAVIOR OF SURFACTANTS ON ZINCOXIDE SURFACES

Fırat Melih GÜRSOY

Supervised by : Prof. Dr. Sümer PEKER

Chemical Engineering Depatment

Deparment Code : 603.01.00
Presentation Date : 24.09.2009

Bornova-İZMİR

2009

Fırat Melih Gürsoy tarafından Yüksek Lisans tezi olarak sunulan "ADSORPTION AND DESORPTION BEHAVIOR OF SURFACTANTS ON ZINCOXIDE SURFACES" başlıklı bu çalışma E.Ü. Lisansüstü Eğitim ve Öğretim Yönetmeliği ile E.Ü. Fen Bilimleri Enstitüsü Eğitim ve Öğretim Yönergesi'nin ilgili hükümleri uyarınca tarafımızdan değerlendirilerek savunmaya değer bulunmuş ve 24/09/2009 tarihinde yapılan tez savunma sınavında aday oybirliği/~~oyçokluğu~~ ile başarılı bulunmuştur.

Jüri Üyeleri:		**İmza**
Jüri Başkanı	**: Prof. Dr. Sümer PEKER**	.....
Raportör Üye	**: Prof. Dr. Mustafa DEMİRCİOĞLU**	.....
Üye	**: Doç. Dr. Fehime ÖZKAN**	.....

ÖZET

YÜZEYAKTİF MADDELERİN ÇİNKOOKSİT YÜZEYLERE ADSORPSİYON VE DESORPSİYON KOŞULLARININ İNCELENMESİ

GÜRSOY, Fırat Melih

Yüksek Lisans tezi, Kimya Mühendisliği Bölümü
Tez Yöneticisi: Prof Dr. Sümer Peker
Eylül 2009, 85 sayfa

Bu çalışmanın amacı, yüzey aktif maddelerin çinko oksit üzerine adsorpsiyon ve desorpsiyon koşullarının incelenmesidir. 104 M 382 TUBİTAK projesi kapsamında üretilen ZnO (çinko oksit) nanotanelerin birbirlerine yapıştıkları ve yüzeylerinin ince bir film tabakası ile kaplandığı görülmüştür. Farklı çözgenlerle yıkamalar yapıldıktan sonra dahi, yüzeyde SDS (sodyum dodesil sulfat)'in kaldığı, SEM görüntüleri ve EDS analizlerinden anlaşılmıştır. Etkileyen parametreleri aydınlatabilmek için ZnO'in üzerine SDS adsorpsiyonu bu çalışmada sistematik olarak incelenmiştir.

Adsorpsiyon katı-sıvı arasında gerçekleştiği için adsorplayan katı ZnO'in sulu çözelti içerisindeki yüzey yapısı, ve adsorplanan SDS'in sulu çözelti içerisindeki özellikleri incelenmiştir. ZnO'in yüzey yapısının ve yüzey yükünün pH ile değiştiği saptanmıştır. Deneysel çalışmalar sonucunda çinko oksitin yüzey yükünün sıfır olduğu noktanın (pzc) elektrolit konsantrasyonuna bağlı olarak $8.7 < pH < 11$aralığında olduğu bulunmuştur. $pH < 8.7$ de yüzey yükü pozitif, $pH > 11$'de negatif olduğu saptanmıştır. Su içerisinde ZnO yüzeylerinde hidroksil gruplarının oluştuğu ve bu grupların ZnO'in $7.75 < pH < 12$ aralığında değişim gösterdikleri bulunmuştur. Çinko oksit'in çözünürlüğü $3 < pH < 12$ aralığında minimumdur. Yüzey yüküne bağlı olarak pH azaldıkça, ZnO yüzeyleri (+) yüklü oldukları için (-) yüklü DS^- (dodesil) iyonlarının adsorpsiyonu artmıştır. Değişik pH değerlerindeki SDS adsorpsiyonu sırasında, çözeltinin pH'ında değişim gözlenmektedir. Bu değişim ZnO yüzeyindeki H^+ ve OH^- iyonlarının yerdeğişimine bağlanmıştır. pH=12 değerinde yüzey yükünün sıfıra yakın olduğu için adsorpsiyon sırasında pH değişimi olmamıştır. pH=12 deki adsorplanan miktar diğer pH'lardakine göre çok fazladır. Bu fazlalık adsorpsiyon mekanizmasının değiştiğini göstermektedir.

Desorpsiyon yüzdesi pH ile artış göstermiştir. Desorplanan SDS miktarı nanotane üretiminde desorplanan miktara göre %50 daha fazladır. Aradaki farkın nanotane üretimi esnasında O- (oksijen) boşluklarına takılarak adsorplanan ve yıkama ile giderilemeyen SDS den kaynaklandığı düşünülmektedir.

Anahtar kelimeler: SDS, adsorpsiyon, pH etkisi, yüzey yükü, yüzey alanı, iletkenlik.

ABSTRACT

ADSORPTION AND DESORPTION BEHAVIOR OF SURFACTANTS ON ZINCOXIDE SURFACES

GÜRSOY, Fırat Melih

Masters Thesis, Chemical Engineering Department
Supervisor: Prof Dr. Sümer Peker
September 2009, 85 pages

The aim of this thesis is the investigation of the adsorption and desorption conditions of surfactants on zinc oxide surfaces. The nanoparticles of ZnO produced in the Project supported by TÜBİTAK under the Technological Research Grant 104M382 were found to be coated by a thin film that caused the particles to stick together. SEM photographs and EDS analysis showed that SDS stil remained on the surfaces even after repeated washings with water and other organic solvents. In this work, SDS adsorption on ZnO is investigated systematically to elucidate the factors controlling the adsorption.

Since adsorption takes place at the solid/liquid interface, the surface composition of the solid ZnO and the physical properties of SDS in solution are investigated. It was found that the surface composition and surface charge of ZnO varied with pH. The point of zero charge was found to vary in the range, $8.7 < pH < 11$, depending on the concentration of the electrolytes. The surface charge of ZnO was found to be positive for $pH < 8.7$ and negative for $pH > 11$. The surfaces of the ZnO particles were found to hydrolyze to different hydroxides of Zn. The pH of the supernatant showed a variation with time in the range $7.75 < pH < 12$. The pH of the solution did not change with time outside this range. The solubility of ZnO is minimum in the interval$3 < pH < 12$. Since ZnO surfaces have a (+) charge below the isoelectric point, the adsorption of negatively charged DS^- increased with a decrease in pH. During the adsorption of SDS at different pH values, the pH of the solution was found to be instable. This variation was attributed to the exchange of H^+ and OH^- ions at the surface. Since the surface charge of ZnO is nearly zero around pH=12, there was no change in the pH of the supernatant solution during the adsorption process. The specific adsorption (mol/g) at pH=12 is much larger than that at other pH values. This excess in

adsorption was attributed to a change in the adsorption mechanism. The percent desorbed from the surfaces was found to increase with pH. In fact, the percent desorption found in this work is about 50% greater than the desorption percentage during the washing step of the nanoparticle production. The difference in the desorbed amounts could be due to the SDS chemically bonded into the O- vacancies during the formation of ZnO nanoparticles, that could not be removed during the washing step.

Keywords: SDS, adsorption, pH effect, surface charge, surface area, conductivity.

ACKNOWLEDGEMENT

I would like to thank to Prof. Dr. Sümer Peker for her support, help and interest throughout this study.

I would also like to thank Prof. Dr. Şerife Helvacı for her help and interpretation about my questions.

I would like to thank to my father Hüseyin Metin Gürsoy, my mother Hafize Gürsoy and all members of the famiy for their help, spiritual and material supports throughout this study. I also owe a thank you to my elder sisters and their husbands Alev Canan Balcı, Murat Balcı and their newborn daughter who is my first niece Nevin Duru Balcı. Also I want to thank to Gül Reva Öztürk and Adem Yavuz Öztürk for their moral support and adoptive support. I would like to thank to my cousins, Emre Yılmaz, Mehmet Yılmaz, Serkan Çağlasın and Miray Apak for not leaving me alone in İzmir. I also owe a thank to my fiancee, Cansu Özkan and her family for their spiritual and material supports and help throughout this study. I would also like to thank Ercan Aksoy and his family for their help and adoptive support during this study.

Furthermore, I remember respectfully to my beloved brother Kadir Alp Gürsoy, my beloved grandfather Kadir Gürsoy, my mother's uncle Hasan Yılmaz, my fatherinlaw Mustafa Kenan Özkan, my aunt's husband Coşkun Halil Baykal, my neighbour Sıtkı Kaleli and his boy Burak Kaleli.

I would like to thank to TÜBİTAK for the scholarship support to me and financial support through project 104 M 382.

I would like to thank Scientific Research Fund of Ege University for the financial support through Project 2009/Muh/048.

TABLE OF CONTENTS

Page

TABLE OF CONTENTS (continued)

Page

TABLE OF CONTENTS (continued)

Page

TABLE OF CONTENTS (continued)

Page

LIST OF FIGURES

Figure **Page**

LIST OF FIGURES (continued)

Figure **Page**

LIST OF FIGURES (continued)

Figure **Page**

LIST OF FIGURES (continued)

Figure **Page**

LIST OF FIGURES (continued)

Figure **Page**

LIST OF TABLES

Table **Page**

1. INTRODUCTION

The subject of the research on which this thesis work is based arises from a problem encountered in the production of ZnO by the microemulsion method in the technological research, Project 104 M 382 supported by TÜBİTAK. ZnO nanorods were grown in a basic medium (pH 13) starting from $Zn(OH)_4^{2-}$ precursor through the reaction,

$$2Na^+ + Zn(OH)_4^{2-} \rightarrow ZnO + H_2O + 2Na^+ + 2OH^-$$

The reaction took place inside the rod-like micelles of hexanol/SDS surfactants dispersed in heptane. The reactions took place at 140^{o}C in an autoclave. At the end of the reaction the nano rod suspension was washed repeat in hot water and the solvents listed in Table 1.1

Table 1.1 Desorption effect of different solvents.

No	Solvents	Initial SDS Amount (10^{-3} mol)	Amount of SDS in washed water (10^{-3} mol)	Desorption of SDS from surfaces, %	% Adsorbed on ZnO surfaces
1	Acetone	3.26	0.10	3.1	96.9
2	Ethanol	3.26	1.01	31.0	69.0
3	Water	3.26	1.56	47.8	52.2
4	Ethylether	3.26	0.05	1.7	98.3
5	Acetonitrile+Water	2.46	0.73	29.5	70.5
6	Ethanol+Water	2.46	0.68	27.8	72.2
7	Acetone+Water	2.46	0.65	26.4	73.7
8	Ethylether+Water	2.46	0.70	28.5	71.5
9	Acetonitrile	3.26	0.08	2.3	97.7
10	Water (again)	3.26	1.36	41.8	58.2

The total amount of SDS in the wash waters were analyzed. The difference of the initial amount of SDS and that analyzed, gave the amount of SDS that remained adsorbed on the surfaces of ZnO nanorods.

That SDS could not be thoroughly removed from ZnO surfaces were further supported by SEM images given in Fig. 1.1. A fluffy film covering the nanorods and the rods joined by the aggregation of these films is clearly evident from Figure 1.1(a-e).

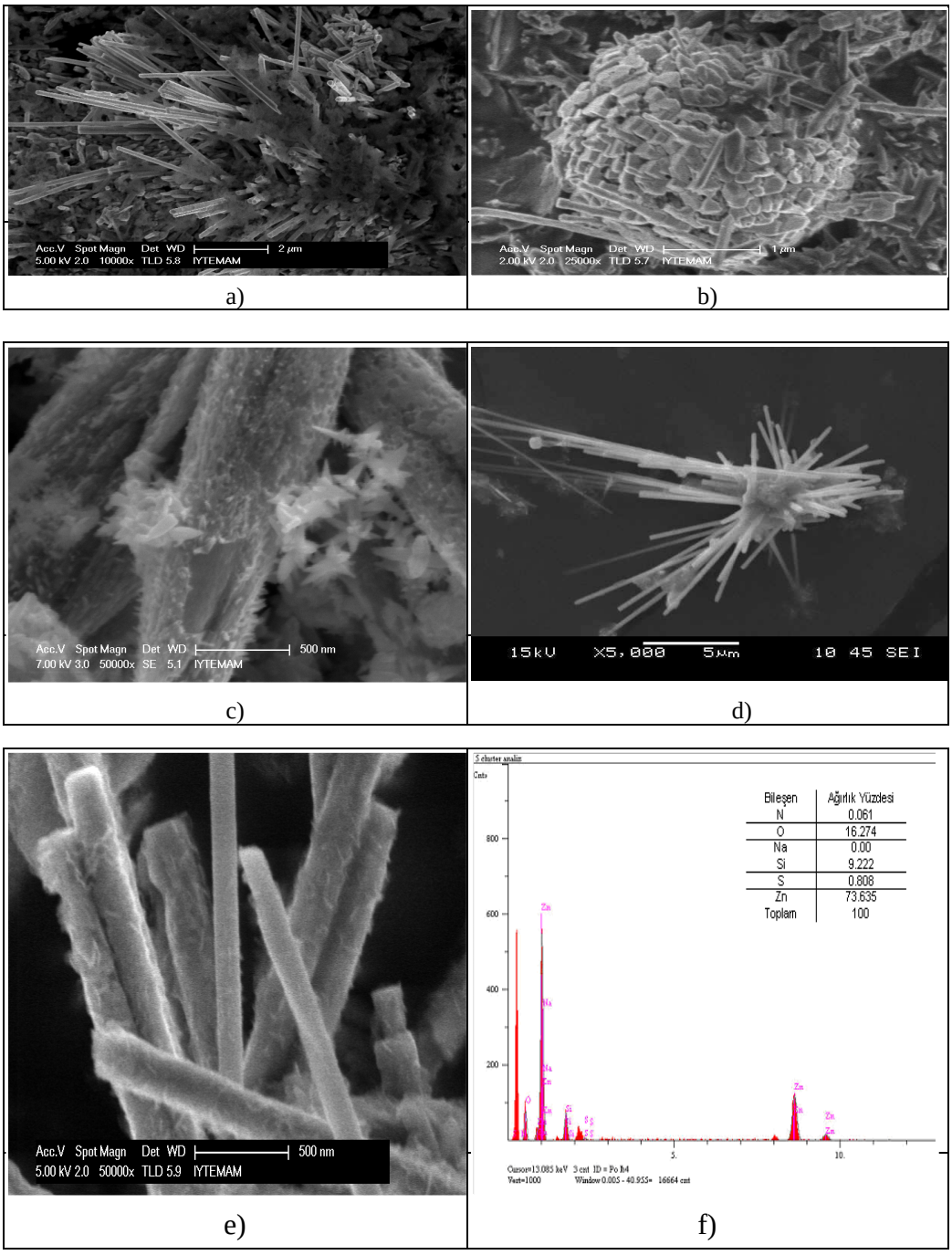

Figure 1.1 SEM and EDS analysis of nanorods.

EDS analysis are made a section the surface of the rods confirm that there is an appreciable amount of S, signifying the presence of SDS.

SDS is a anionic surfactant molecule has the chemical composition $C_{12}H_{25}OSO_3^-.Na^+$ and the structural formula is illustrated in Fig. 1.2.

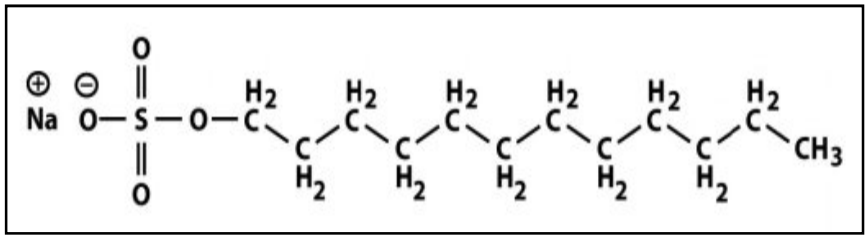

Figure 1.2 Structure of SDS.

The molecule consists of a long, eleven-unit methylene (CH_2) chain, terminated on the right-hand end with a methyl (CH_3) group. This chain is the nonpolar tail. The left-hand end terminates with the sulfate polar headgroup. In polar solvents like water this amphiphilic molecule ionizes to form an anionic amphiphile and a sodium cation. The negatively charged hydrophilic polar headgroup $(O\text{-}SO_3)^-$ is attracted to the water molecules while the hydrophobic tail is repelled.

ZnO is considered as one of the industrially important metal oxides with a wide range of application areas, due to its optical, electrical and mechanical properties. ZnO normally forms in the hexagonal (wurtzite) crystal structure (Fig. 1.3). HCP packing of oxygen anions (black) produces the ZnO wurtzite structure of zinc oxide. The co-ordination of Zn is tetrahedral, because there is little energy difference between the tetrahedral and hexagonal structures.

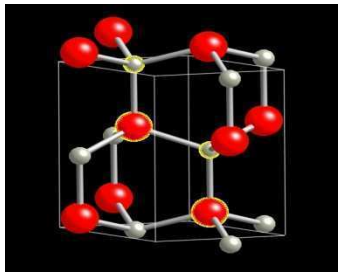

Figure 1.3 Wurtzite structure of ZnO (Zn grey, O black).

The appearance of Si on the surfaces must be due to a calibration error of the instrument for there were no silicates in the reaction mixture and the each water. Na peak coincides with the Zn peak and therefore could not be analyzed. It is more probable that Na^+ ions were removed from the surfaces by washing, after the adsorption of SDS.

Aim of this research is to determine the adsorption and desorption behaviour of SDS onto ZnO surfaces. In addition, characterization of ZnO surfaces structure in the aqueous solution. Since ZnO nanoparticles' produced in the Project (TUBITAK 104 M 382) was not sufficient in amount for the analyses, ZnO, from Merck was used. ZnO from Merck was characterized by the same methods used for the ZnO obtained in the project.

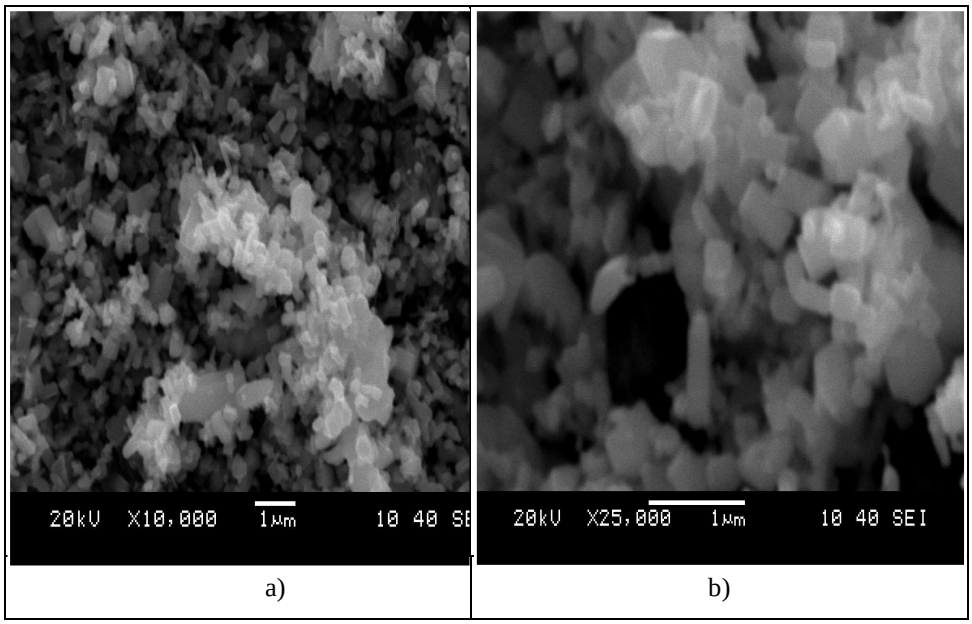

Figure 1.4 SEM images of Merck ZnO.

SEM images of Merck's ZnO showed that the particles were short with cylinders with hexagonal cross-sections (Fig. 1.4). Their dimensions were in the order of nanometers. So, we decided Merck ZnO could be used to simulate the ZnO produced in the project.

Although SDS in extensively used in research, literature on the adsorption of SDS on ZnO is scarce. The relevant literature on the subject is summarized in Table 1.2.

Table 1.2 Several researches about SDS adsorption.

Author, year	Adsorbate	Adsorbent	Parameter	Main results
Sadowski and Polowezyk, 2004	SDS-anionic surfactant CTAB-cationic surfactant	ZnO, IEP:8.95	ZnO-BET surface Area: 5.75 m^2/g pH: not adjusted. T: 20^oC	CTAB, increases the zeta potential and exhibits higher adsorption. SDS, decreases the zeta potential.
Sadowski and Polowezyk, 2004	SDS-anionic surfactant CTAB-cationic surfactant	MgO, IEP:12.4	MgO-BET surface area: 8.4 m^2/g pH: not adjusted. T: 20^oC	CTAB, increases the zeta potential. SDS, decreases the zeta potential and exhibits higher adsorption.
Tulpar and Ducker, 2004	SDS-anionic surfactant	Gold-thiol	Surface charge of Gold-thiol, controlled and fixed density. SDS, recrystallized ethanol. Salt: NaCI Water,deionizd, charcoal-filtered T,constant. pH,constant.	Adsorption, independent of the surface charge density. First, formation of a bilayer of surfactant molecules.Second, opposite orientation of the molecule. Charge regulation, removes the counterion from the surface. NaCL, decreases the interaction
Hu and Bard, 1997	SDS-anionic surfactant	Gold-thiol	Surface charge of Gold-thiol, controlled and fixed density. SDS,purified by recrystallization from ethanol to remove any impurities. Water,deionized T,constant.	CMC, 8.1-8.4mM Surface,positively charged. Addition of SDS,surface charge reversal to negative charge on substrate and SDS form bilayer film or small surface micelle. Surface charge is related to the amount of SDS adsorbed on the substrate. Near the CMC,monolayer adsorption, greater than CMC,bilayer adsorption and micelle structure.

<table>
<tr><td rowspan="3">Levchenko et al., 2002</td><td>SDS</td><td>Gold-thiol</td><td colspan="2">Surface charge of Gold-thiol, controlled and fixed density. SDS purified recrystallization from ethanol to remove any impurities. Purified water was from a NanoPure system.</td></tr>
<tr><td colspan="4">Main results</td></tr>
<tr><td colspan="4">Surface, positively charged. Purity of SDS plays a significant role. Sodium dodecyl sulfate is known to hydrolyze over time to form dodecanol which enhances the adsorption of SDS below the critical micelle concentration (cmc) (8.1mM) and decreases the adsorbed amount above the cmc. The dodecanol impurity can exist in commercially available SDS purity on SDS adsorption equilibria. A decrease in the adsorbed amount of surfactant above the cmc can be associated with solubilization of dodecanol in SDS micelles in the bulk. Dodecanol lead to max. adsorption above the cmc. Adsorption depends on SDS concentration. Below the cmc, the kinetics of ionic surfactant adsorption is governed by monomer adsorption. Above the cmc, where micelles are present the mechanism of surfactant adsorption can depend on the nature of the surface. The micelles should not be able to adsorb directly onto hydrophobic surface. If the surface is hydrophobic, intermolecular van der Waals forces stabilize adsorption. In the case of charged hydrophilic surfaces, the electrostatic forces are also involved and dominate the interaction compared to the van der Waals forces.</td></tr>
<tr><td>Purakayastha et al., 2005</td><td>SDS, anionic surfactant</td><td>Rubber granules</td><td>Double distilled water was used. Rubber granul-BET:0.45-0.78 (m^2/g) and washed with distilled water, dried at 103^{o}C for 2h. pH: 6
T: 26^{o}C</td><td>Rubber granules could remove up to %92 of SDS from wastewater. Langmuir and Freundlich adsorption isotherms were usud. Adsorption of more strongly sorbing solute, the adsorption would be controlled by pore diffusion.</td></tr>
<tr><td rowspan="4">Schulz and Warr, 2002</td><td colspan="2">Adsorbate</td><td>Adsorbent</td><td>Parameter</td></tr>
<tr><td colspan="2">SDS-cmc: 8.2E-3M
TTAB-cmc: 3.6E-3M
CTAB-cmc: 9E-4M</td><td>-Titanium dioxide (rutil).
-Quartz.
-Kaolinite.</td><td>Milli-Q water was used.
The particles were dried at 130^{0}C for 15min.</td></tr>
<tr><td colspan="4">Main results</td></tr>
<tr><td colspan="4">TTAB and CTAB adsorption onto quartz, the nearest neighbor distances of the aggregates within the adsorbed layer, which decrease significantly with increasing pH for both CTAB and TTAB. SDS and TTAB adsorption onto rutil,at pH:3.3, 4.1, 5.2, a periodic texture is observed, indicating that SDS forms spherical org lobular surfactant aggregates. Significant adsorption of SDS was observed at pH 3, whereas the amount adsorbed at pH 10 was insignificant. In contrast, CTAB adsorbs at both pH values, with greater adsorption at pH 10. The adsorption behavior of SDS was attributed to the charge on the edges of kaolinite particles. Adsorbed micelles of SDS are found at pH's less than the point of zero charge of rutile, whereas TTAB and CTAB adsorbed micelles are found only above the points of zero charge of rutile and quartz,respectively.</td></tr>
</table>

2. THEORY

Adsorption depends on many parameters, such as the surface morphology and characterization of the adsorbate, molecular structure of the adsorbent, its solubility and critical micelle concentration and physical properties of the liquid solvent. For this reason investigation of the rate of adsorption, without studying the effective parameters has little significance and remains empirical.

2.1 Interfacial Properties of SDS

Surfactants are amphiphilic molecules that possess both hydrophobic and hydrophilic properties. A typical surfactant molecule consists of a long hydrocarbon 'tail' that dissolves in hydrocarbon and other non-polar solvents, and a hydrophilic 'head-group' that dissolves in polar solvents (typically water). The nature of the head group makes it possible to divide surfactants into subclasses namely: Anionic, Cationic, Zwitterionic and Nonionic. One example of a dual-character molecule having a polar head-group and a non-polar tail is sodium dodecyl sulphate (SDS, anionic surfactant), $NaOSO_3C_{12}H_{25}$ (Fig.2.1).

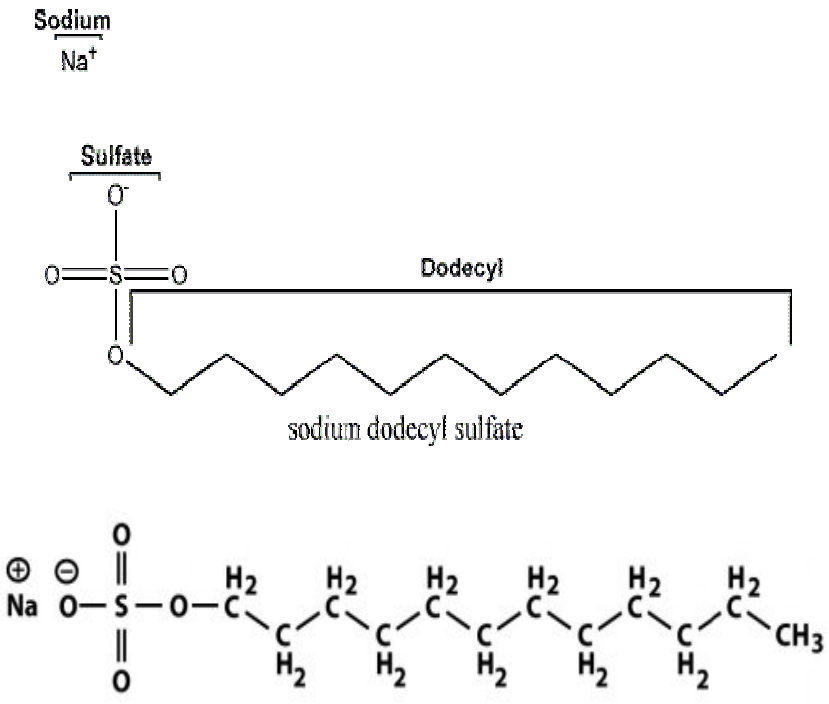

Figure 2.1 Typical structure of SDS (Stokes and Evans, 1996).

When a sufficient amount of SDS is dissolved in water, several bulk solution properties are significantly changed, particularly the surface tension

(which decreases) and the ability at the solution to solubilise hydrocarbons, (which increases). These changes do not occur until a minimum bulk SDS concentration is reached. This concentration is called the critical micelle concentration (CMC).

Technically, a micellar solution is a colloidal dispersion of organised (self-assembled) surfactant molecules (Fig.2.2). Non-ionic surfactant molecules can cluster together in micelles of 1000 molecules or more, but ionic species tend to form micelles with 10 to 100 molecules because of electrostatic repulsions between the head-groups.

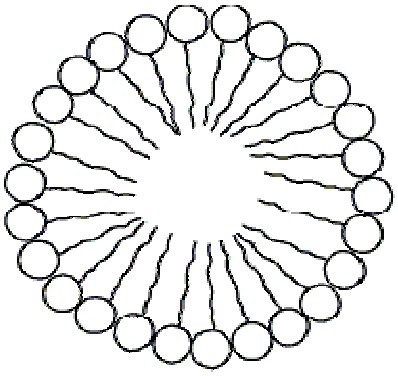

Figure 2.2 Micelle structure of SDS (Chen et al., 2009).

2.1.1 Conductometric determination of the cmc

Below the CMC, the addition of surfactant to an aqueous solution causes an increase in the number of charge carriers (Na^+ (aq) and $^-OSO_3C_{12}H_{25}$ (aq)) and consequently, an increase in the conductivity. Above the CMC, further addition of surfactant increases the micelle concentration remains approximately constant (at the CMC level) (Fig. 2.3). A plot of conductivity against surfactant concentration is, thus expected to show a break at the CMC (Stokes and Evans, 1996; Huang and Lee, 2001).

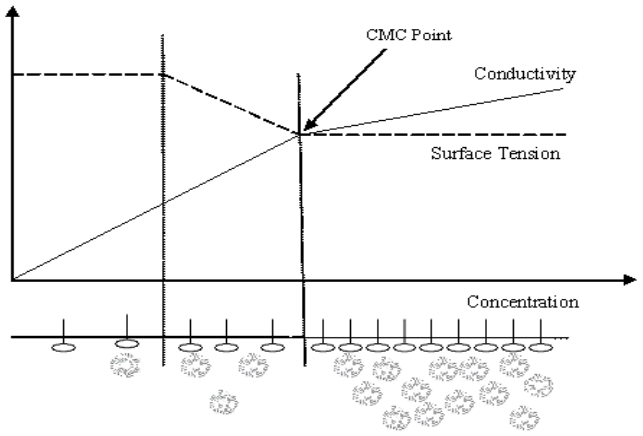

Figure 2.3 Demonstration of CMC point of surfactant (University of Malta, 2000).

Below and above the CMC, surfactants are present in the form of monomers and micelles, respectively. Numerous factors can influence CMC values, including type and concentration of electrolytes, temperature, surfactant structure, and organic additives.

2.1.2 Micellar geometry and critical packing parameter

At low bulk concentrations surfactant molecules are present in aqueous solutions as solvated monomers. However, when their bulk concentration exceeds a critical value, known as the critical micelle concentration (CMC), the hydrophobic tails segregate from water and aggregate into colloidal micelles with a hydrophobic interior and a hydrophilic surface. The shape of micelles is determined by the critical packing parameter, CPP defined as

$$\mathrm{CPP} = \frac{\mathrm{V_{tail}}}{\mathrm{L_{tail} * a_o}} \tag{2.1}$$

a_o= The mean molecular area occupied by a surfactant molecule.

$\mathrm{L_{tail}} = \left[1.5 + 1.265\left((\mathrm{n_c} - 1) - \mathrm{x}\right)\right]$ Length of the tail. (2.2)

n_c = The number of carbon atoms in the hydrocarbon chain in the tail.

$\mathrm{V_{tail}} = \mathrm{n_{HC}}\left[\left((\mathrm{n_c} - 1) - \mathrm{x}\right)\mathrm{V_{CH_2}} + \mathrm{V_{CH_3}}\right]$ Volume of the hydrocarbon tail. (2.3)

$\mathrm{V_{CH_2}} = \text{Volume of the } CH_2.$

V_{CH_3} = Volume of the CH_3.

n_{CH} = The number of hydrocarbon atoms in the hydrocarbon chain in the tail.

x = Variation of Length, i.e. full length or reduced length.

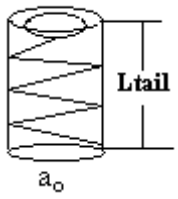

Figure 2.4 Shape of a surfactant molecule (Jönsson et al, 1999).

The area, a_o includes water molecules in the hydration shell of the polar head and the effects of electrostatic repulsion. Spherical micelles are formed for CPP ≤ 0.33, globular or spherocylindrical micelles for 0.33 < cpp < 0.5 and vesicles for CPP > 0.5. SDS has a long hydrocarbon chain and the packing parameter of SDS is 0.37. It forms spherical micelles (Fig.2.5) and depending on the concentration, ionic strength of the solution and the nature of the counterion the shape of its micelles may vary from spherical to spherocylindrical (Rieger and Rhein, 1997).

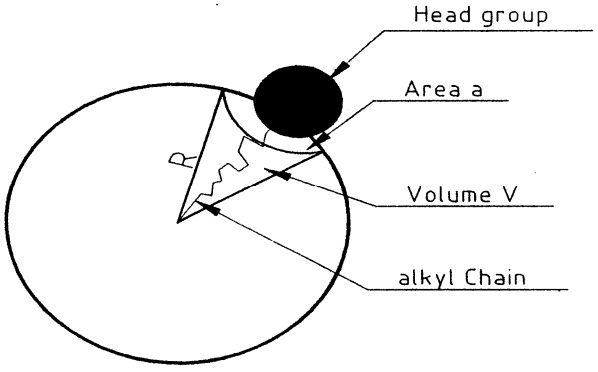

Figure 2.5 Schematic representation of an idealized spherical micelle.

2.2 Structure of ZnO Particles

Zinc oxide is a chemical compound with the formula ZnO. It is nearly insoluble in water but soluble in acids and alkalis. It occurs as white hexagonal, wurtzite type crystals and a white powder commonly known as zinc white (Fig. 2.6). Zinc oxide occurs in nature as the mineral zincite. Physical and chemical properties and crystal structure data of ZnO are given in Table 2.1and 2.2.

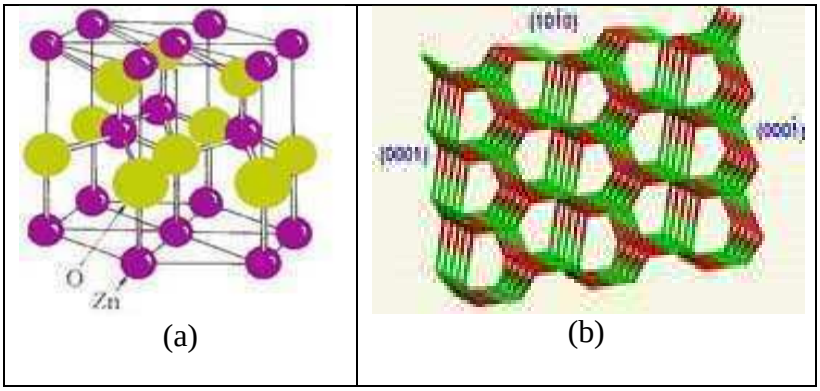

Figure 2.6 (a) The crystal structure of ZnO (hexagonal), (b) the face of ZnO crystal.

Table 2.1 Physical characteristic of ZnO (Zhuxi, 1995).

Crystal Structure	Hexagonal ,Wurtzite.
Lattice parameters	a=3.249Å, c=5.205Å, c/a=1.602
Melting temperature	1975 ^{o}C
Density	5676 kg/ m^{3}
Specific heat	0.125 kal/g
Thermal conductivity	0.006 kal/cm/K
Thermoelectric constant	1200 mV/K at 573 K

Table 2.2 Crystal structure data (Zhuxi, 1995).

Spacegroup Symbol:			P 63 m c		
Origin Offset:			(none)		
Lattice Type:			P		
Unit Cell Parameters					
a [A]	**b [A]**	**c [A]**	**alpha [deg]**	**beta [deg]**	**gamma [deg]**
3.3500	3.3500	5.2200	90.000	90.000	120.000
Fractional Coordinates of Atoms in the Asymmetric Unit					
Site Label	**Element**	**x**	**y**	**z**	
O	O	0.3333	0.6667	0.3750	
Zn	Zn	0.3333	0.6667	0.0000	

Zinc oxide is a rather common material which is used for a quite large variety of different applications. Probably the most ‘‘visible’’ use in every day’s life is that as a white pigment (zincwhite) in painting and coloring of e.g. paper. A completely different area is medicine, where zinc oxide is used e.g. in wound-treatment making use of its antiseptic properties. In addition to these applications dating back to previous centuries the present technological importance of ZnO results from its semiconducting and optical properties. One example are transparent conducting oxide (‘‘TCO’’) layers which are suitable to be used as

front electrodes in thin film solar cells. ZnO has also been used as a sensor for hydrogen and carbon hydrides since the conductivity of thin zinc oxide films varies considerably with hydrogen gas pressure.

Presently, the possibility to grow ZnO nanoparticles in a rather large variety of sizes and shapes is attracting considerable attention. With regard to chemical processes one of the oldest applications is in connection with rubber vulcanisation. ZnO has been used to accelerate sulphur-induced vulcanisation and to improve the properties of rubber.

2.2.1 Structure of ZnO crystals

ZnO crystallizes in the wurtzite structure with each O^{2-} ion surrounded by a tetrahedron of four Zn^{2+} ions, and vice versa. In an ionic crystal of zinc oxide in which the oxide ions are greater than 1.5 times the diameter of the zinc, the smaller zinc ions may retreat to semi-interstitial locations just beneath the surface where they are shielded from complete surface exposure (Fig. 2.7a). The structure lacks inversion symmetry and cutting the crystal perpendicular to the c-axis results in two structurally different surfaces. Hence the two opposite sides of the c-oriented wafer are terminated with one type of ions only. These polar, or 'basal', surfaces (bases of the prism shown in Fig. 2.7b) are usually referred to as (0 0 0 1)-Zn and (0 0 0 $\bar{1}$)-O terminated surfaces.

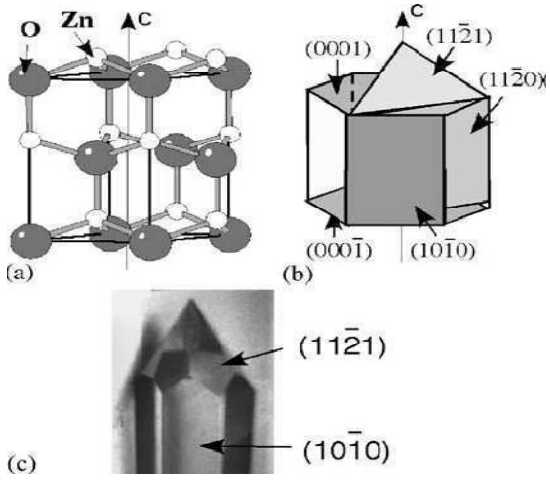

Figure 2.7 a) Unit cell of the ZnO wurtzite crystal structure, b) lowindex planes of the crystal, c) photograph of a ZnO single crystal grown with the VT method.

The (1 0 $\bar{1}$ 0) and (1 1 $\bar{2}$ 0) and surfaces are the prism faces and the (1 1 $\bar{2}$ 1) surface is the pyramid face of the crystal. Fig. 2.7c shows a photograph of a 'pencil'-type ZnO single crystal grown from the vapor phase, with the (1 0 $\bar{1}$ 0) and (1 1 $\bar{2}$ 1) faces labeled (Diebold et al., 2004).

The internal structure of a crystalline solid as a perfect array of atoms or ions reproduced indefinitely is not accurate. Many breaks in the perfect periodicity lead to well-defined imperfections.

The regularity in a single-phase, pure, single crystalline solid can be broken by:

1. Point imperfections, such as vacancies and interstitials exist in thermodynamic equlibrium. Surfaces act as source and sink for vacancies. Point imperfections in ionic solids are charged (zero-dimension imperfections).

2. Linear imperfections, such as dislocations are introduced by thermal/mechanical stress. Edge dislocations lie perpendicular, screw dislocations parallel with their Burgers vector (one-dimensional imperfections).

3. Planar imperfections, such as small-angle boundaries, stacking faults, twins have surface energy (two dimensional imperfections).

4. Volume imperfections, such as voids (three-dimensional imperfections).

2.2.1.1 Non-polar surfaces of ZnO

The mixed-terminated (10$\bar{1}$0)-surface

The ZnO (10$\bar{1}$0)- mixed-terminated surface of zinc oxide is the energetically most favorable surface; SEM images recorded for ZnO powder particles reveal a dominance of this surface which forms the sides of the hexagonal columns, see Fig. 2.8.

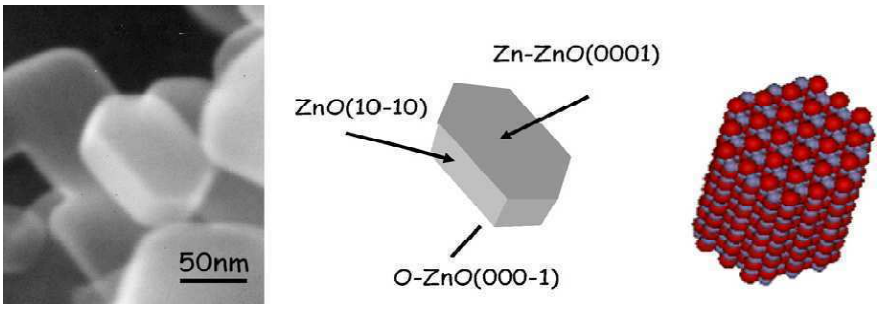

Fig.2.8 Left: SEM-image of ZnO powder particles. Center: schematical sketch showing the typical shape of ZnO powder particles, a hexagonal column with the top-face corresponding to the Zn-terminated Zn–ZnO surface and the bottom to the O-terminated O–ZnO surface. The six side faces are all equivalent and correspond to the mixedterminated ZnO $(10\bar{1}0)$ surface. Right: Atomic model of a hexagonal column of a ZnO particle (Wöll, 2007).

The nonpolar surface is not electrostatic instabilities as expected for the polar surfaces are present and the actual geometric structure of the surface should be similar to a bulk truncation, which is illustrated in Fig. 2.9

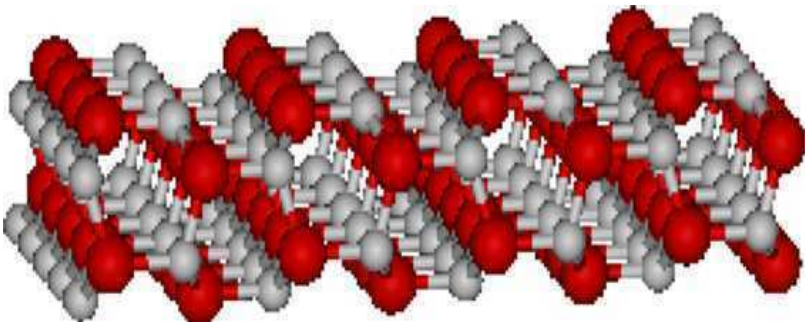

Figure 2.9 Structure of a bulk-truncated mixed-terminated ZnO $(10\bar{1}0)$ surface. The Zn atoms are represented by the grey, small balls, the oxygen atoms by the black balls. Unlike the two polar surfaces of ZnO, O–ZnO and Zn–ZnO, this unpolar surface does not exhibit an electrostatic instability (Wöll, 2007).

Today, in terms of industrial added value, the chemical properties of ZnO surfaces are the most important ones. Many different chemicals are produced using zinc oxide or zinc oxide based compounds as a heterogeneous catalyst. The most prominent example is methanol, which until 1960 has been produced with catalysts containing ZnO as the active component. Although there has been a substantial interest recently in unravelling the atomistic mechanisms on the ZnO catalysts, the only consensus appears to be that O-defects are the active sites.

In the surface tunnelling microscopy (STM) micrographs shown in Fig. 2.10 it is remarkable that the density of defects aside from step edges, in particular that of vacancies, is fairly low. In the study by Wöll (2007) this question has been investigated in some more detail and on the basis of the STM data it was proposed that on the clean ZnO $(10\bar{1}0)$ surface only few defects exist which correspond to missing oxygen atoms or missing ZnO pairs. In the same work it was reported that after exposure to hydrogen the number of defects increases substantially and both oxygen vacancies as well as ZnO vacancies can be observed.

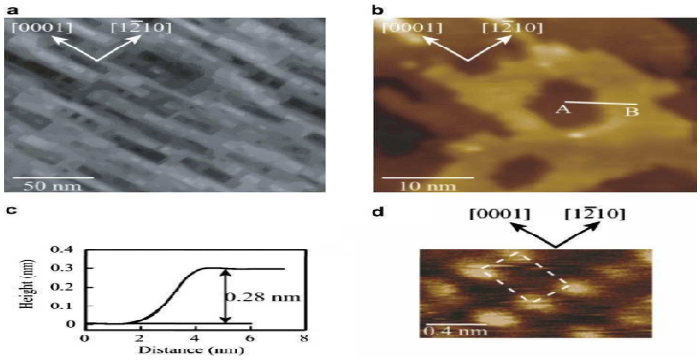

Figure 2.10 STM images recorded for a clean, mixed-terminated ZnO (1 0 $\bar{1}$ 0) surface. The large scale image shown in (a), width 200 nm, was obtained at room temperature, images (b) and (d) were obtained at 380–400 K, tunneling parameters: 2.1 V, 1.3 nA in (a), 2.6 V, 0.4 nA in (b) and 0.7 V, 1.1 nA in (d); (c) line profile AB indicated in b. Figure taken from (Wöll, 2007).

The mixed-terminated $(11\bar{2}0)$-surface

This nonpolar surface has been the subject of a few studies only; the number of works reported for this termination is significantly smaller than for the other surfaces of ZnO.

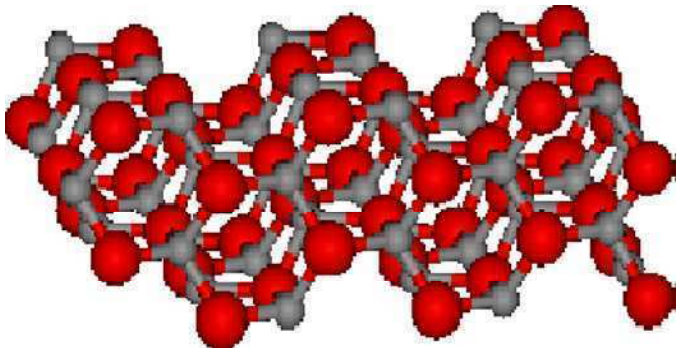

Figure 2.11 Structure of a bulk-truncated mixed-terminated ZnO $(11\bar{2}0)$ surface. The Zn atoms are represented by the grey, small balls, the oxygen atoms by the black balls. Unlike the two polar surfaces of ZnO, O–ZnO and Zn–ZnO, this unpolar surface does not exhibit an electrostatic instability (Wöll, 2007).

The atomically resolved image in Fig. 2.12 shows a sublattice with only one kind of atomin the unit cell. Typically, cations are imaged in empty-states STM of metal oxides, Zn atoms are tentatively assign bright spots. Oxygen vacancies are a common surface defect on metal oxide surfaces and can be observed directly with STM (Libuda and Sicoles, 2000); no indication of missing O atoms was observed in such atomically resolved images on ZnO. Missing 'atoms' in the atomic rows were observed occasionally. This could indicate that either Zn atoms are missing, or that adsorbates sitting on these Zn sites make them appear black. The surface free energy of the ZnO $(10\bar{1}0)$ surface was found to be only slightly larger than for the ZnO $(11\bar{2}0)$ surface, but significantly lower than for the two polar ZnO surfaces.

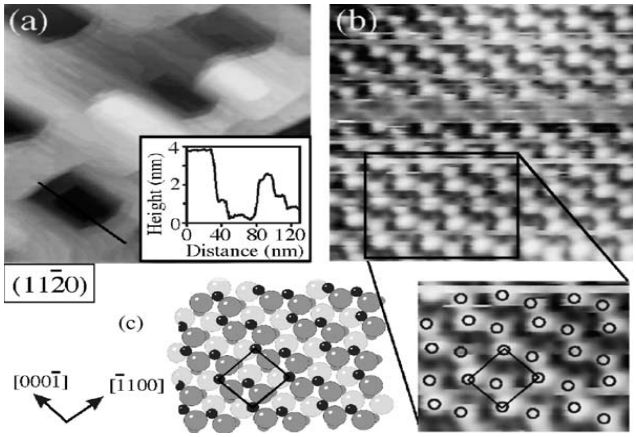

Figure 2.12 Atomic model (white balls O, gray balls Zn) of a (1 x 1) terminated surface (Diebold et al., 2004).

2.2.1.2 The polar surfaces of ZnO

For single crystals of ionic materials with a non-centro symmetric bulk structure a particular type of surface orientations exists which are referred to as polar surfaces. The ideal surface geometry of a polar surface obtained by a simple truncation of the bulk structure with ions of the same formal charge as in the bulk is not stable. This instability of the polar surfaces of ionic crystals scales with the size of the specimens so that, in principle, polar surfaces of very small oxide particles could be stable.

Surprisingly, most previous studies carried out for the two polar ZnO surfaces, the O-terminated O–ZnO surfaces or ZnO $(000\bar{1})$ as well as the Zn-

terminated Zn–ZnO surface (or ZnO(0001)), have failed to observe any reconstruction.

Structure of the zinc-terminated ZnO(0001) surface

The structure of an ideal, unreconstructed and unrelaxed Zn–ZnO surface is shown in Fig. 2.13 a; b.

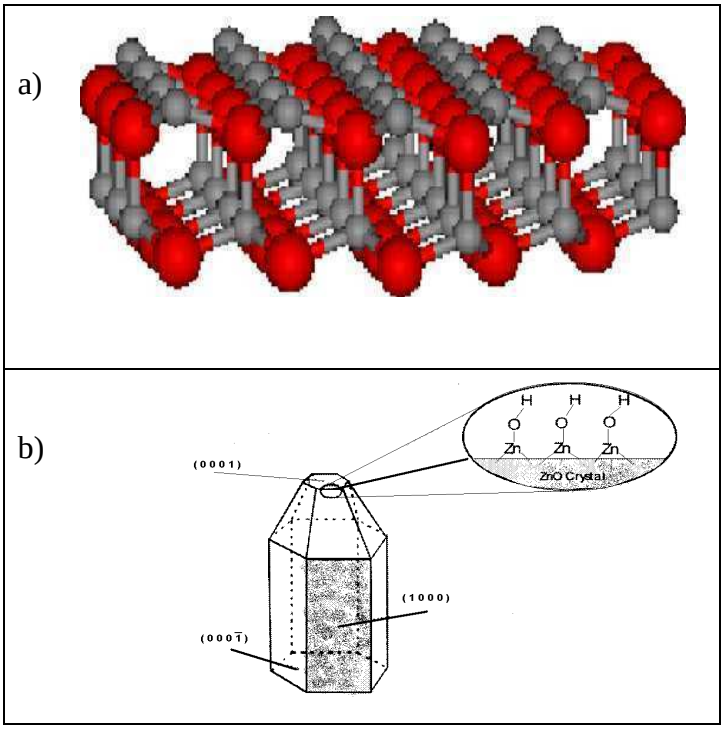

Figure 2.13 a) Structure of an ideal, unreconstructed Zn–ZnO(0001) surface. The Zn atoms are represented by the grey, small balls, the oxygen atoms by the black balls. Note, that this surface is electrostatically instable (Wöll, 2007). b) Polar planes of ZnO (Peterson, 2004)

The observation is general to all diffraction studies and suggests a high density of defects, a typical phenomenon for oxide surfaces. This fact really calls for a microscopy study of this surface. In a recent STM study by Wöll (2007) the nature of theses defects has been identified: the results revealed the presence of a large number of steps resulting in a rather rough surface with many triangular-shaped terraces, yielding a very characteristic morphology (Wöll, 2007), see Fig. 2.14.

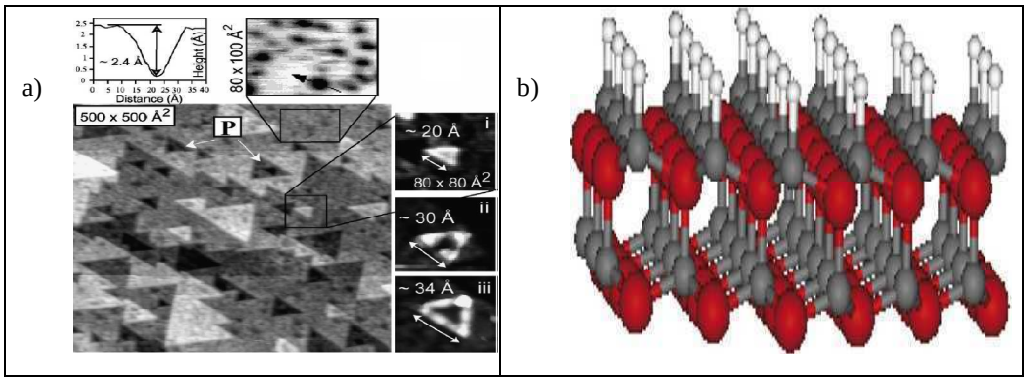

Figure 2.14 a) STM images recorded for a Zn–ZnO surface, from Dulub et al., (2003). b) Structure of the H-saturated H(1 · 1) Zn–ZnO surface. Note, that this surface is electrostatically instable.

As expected from the small size of an H-atom relative to the surface unit cell, the exposure of the zinc-terminated Zn–ZnO surfaces to atomic hydrogen leads to the formation of a H(1 x 1) overlayer.

The polar O–ZnO surface, ZnO (0 0 0 $\bar{1}$)

The structure of an ideal, unreconstructed O–ZnO (0 0 0 $\bar{1}$) surface is shown in Fig. 2.15. The terraces on the O-terminated surface are much smoother than the Zn-terminated surface; no nanosized holes are visible (Diebold, 2004). Since the bulk-terminated (1 x 1) surface should be unstable due to an electrostatic instability, the absence of a structural rearrangement in principle implies the presence of a charge transfer, leading to a metallization of this surface.

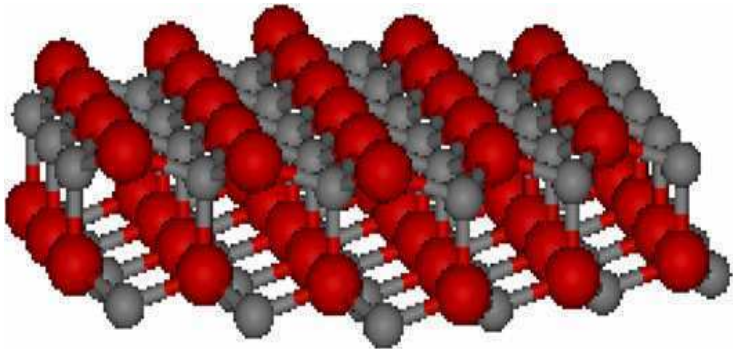

Figure 2.15 Structure of the ideal oxygen-terminated polar surface of ZnO, O–ZnO or ZnO (0 0 0 $\bar{1}$). Note, that this surface exhibits an electrostatic instability.

There are several experimental findings which support such a structural model proposing rows of oxygen vacancies. This surface is always saturated with hydrogen.

2.2.2 Surface structure of ZnO

Many metal oxides will hydrolize in the presence of water to form hydroxide layers at the surface (≡M-OH). Water molecules may be both physically and chemically adsorbed onto the surface of the dispersed oxide particles. The polar hydroxyl (-OH) groups may cause the surface to attract and physically adsorb a single or several additional layers of polar water molecules. An oxide or hydroxide surface (≡M-OH) can become charged by reacting with H^+ or OH^- ions due to surface amphoteric reactions (Eqs. (2.4) and (2.5)).

$$\equiv M - OH + H^+ \leftrightarrow \equiv M - OH_2^+ \quad (2.4)$$

$$\equiv M - OH + OH^- \leftrightarrow M - O^- + H_2O \quad (2.5)$$

At low pH, hydroxide surfaces adsorb protons to produce positively charged surfaces ($\equiv M - OH_2^+$). At high pH they lose protons to produce negatively charged surfaces ($\equiv M - O^-$). The number of these sites and the surface charge of the oxide particles are determined by the pH of the solution. The useful pH range may be limited because the solubility of oxides and hydroxides is strongly pH dependent, especially when the cation can form hydroxyl complexes.

When the zinc oxide is immersed in the water the surface of the oxide is hydrolyzed and a layer of hydroxide is built up (Degen and Kosec, 2000).

A higher solubility of this oxide (ZnO) in comparison to either TiO_2 or Fe_2O_3 complicates potentiometric titration because dissolution processes also compete significantly for added acid or base (Sedlak and Janusz, 2008).

The surface charge is formed on the metal oxide as a result of ionization and completion reaction of surface hydroxyl groups. Surface charge density as a function of pH is very important characteristic of the surface properties of the metal oxide/electrolyte solution (Sedlak and Janusz, 2008).

In aqueous solution ZnO dissolution takes place according to the following reactions:

$$Zn^{2+}_{(aq)} + OH^- \leftrightarrow Zn(OH)^+_{(aq)} \quad (2.6)$$

(2.7)

(2.8)

(2.9)

(2.10)

(2.11)

(2.12)

(2.13)

(2.14)

(2.15)

(2.16)

The solubility diagram for zinc oxide in equilibrium with an aqueous solution at varying pH is shown in Fig. 2.16.

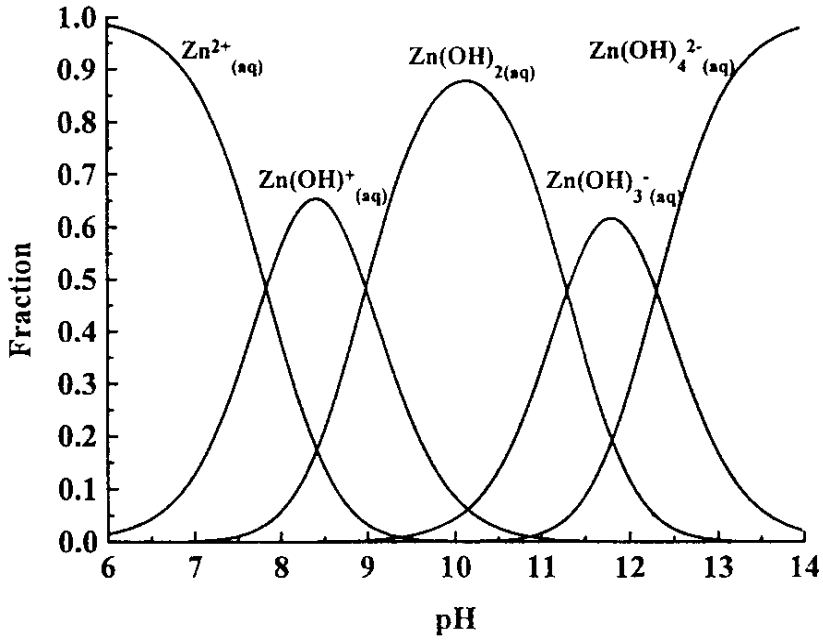

Figure 2.16 Solubility diagram for zinc oxide (Reichle et al., 1975).

In water suspension of zinc oxide the surface hydroxide ≡Zn-OH or $Zn(OH)_{2(s)}$ is in equilibrium with the solution which contains species that can be represented by $Zn^{2+}_{(aq)}$, $Zn(OH)^{+}_{(aq)}$, $Zn(OH)_{2(aq)}$, $Zn(OH)^{-}_{3\,(aq)}$ and $Zn(OH)^{2-}_{4\,(aq)}$. Fig. 2.16 represents the fraction of zinc species existing as $Zn^{2+}_{(aq)}$, $Zn(OH)^{+}_{(aq)}$, $Zn(OH)_{2(aq)}$, $Zn(OH)^{-}_{3\,(aq)}$ and $Zn(OH)^{2-}_{4\,(aq)}$ over a range of pH at 25°C. The hydroxide complexes can be represented by the formula $Zn(OH)_{i}^{2-i},\ i = 1 - 4$, also (Degen and Kosec, 2000).

Amphoteric molecules called zwitterions contain both positive and negative charges depending on the functional groups present in the molecule. The net charge on the molecule is affected by pH of their surrounding environment and can become more positively or negatively charged due to the loss or gain of protons (H^+). The point of zero charge (pzc), in physical chemistry, is a concept relating to the phenomenon of adsorption, and it describes the condition when the electrical charge density on a surface is zero. It is usually determined in relation to an electrolyte's pH, and the pzc value is assigned to a given substrate or colloidal particle. When the pH is lower than the pzc value, the system is said to be "below the pzc." Below the pzc, the acidic water donates more protons than hydroxide groups, and so the adsorbent surface is positively charged (attracting anions). Conversely, above pzc the surface is negatively charged (attracting cations/repelling anions).

The isoelectric point (pI), sometimes abbreviated as IEP, is the pH at which a particular molecule or surface carries no net electrical charge. The pI is the pH value at which the molecule carries no electrical charge or the negative and positive charges are equal.

The pzc is the same as the isoelectric point (IEP) if there is no adsorption of ions other than the potential determining H^+/OH^- at the surface. This is often the case for pure ("pristine surface") oxides in water. In the presence of specific adsorption, pzc and isoelectric point generally have different values.

The point of zero charge (pzc) and isoelectric point of the material can be obtained several methods as (Kosmulski, 2009);

- *cip* (common intersection point of potentiometric titration curves obtained at three or more ionic strengths or equivalent methods).

- *intersection* (intersection point of potentiometric titration curves obtained at two ionic strengths).
- *pH* (natural pH of the dispersion, e.g., mass titration and potentiometric titration at one electrolyte concentration).
- *IEP* (isoelectric point obtained by means of electrophoresis, electroosmosis, or electroacoustic method).

One of the methods used for determination of the point of zero charge is the potentiometric acid-base titration of dispersion. Comparison with blank titration in the absence of the dispersed solid oxide phase yields relative values of the surface charge densities. Absolute values of the surface charge densities are then obtained by setting the zero value at the common intersection point (isoelectric point) for different ionic strengths. The advantage of this method is that experiments can be performed at extremely low ionic strengths.

The basic process at a metal oxide surface in aqueous environment is the surface charging due to interactions of active surface sites with the potential determining ions. For metal oxides, the potential determining ions are H^+ and OH^- ions.

The surface charge density (C/m^2) can then be expressed as

$$\sigma = \frac{\Delta V * M * F}{S * m * 1000} \tag{2.17}$$

where,

ΔV (mL): difference between the titrant volumes used for the solution with ZnO and the electrolyte solution at given pH values.

M (mol/L): molarity of the titrant.

F (C/mol): Faraday constant (96500 C/mol).

S (m^2/g): specific surface area of ZnO.

m (g): mass of ZnO in solution.

2.3 Adsorption

Adsorption at the solid–fluid interface plays a significant role in various disciplines of the natural science and underlies a number of technological processes. The applications of adsorption are widespread; among the many fields of practical importance based on this process, one can mention heterogeneous catalysis, flotation, material science, microelectronics, ecology, separation of mixtures, purification of air and water, electrochemistry, chromatography, and so forth.

2.3.1 Adsorption theories

Adsorption is the adhesion of atoms or molecules on the surface of a material. This process creates a film of the adsorbate (the molecules or atoms being accumulated) on the adsorbent's surface. It is different from absorption, in which a substance diffuses into a liquid or solid to form a solution. The term sorption encompasses both processes, while desorption is the reverse process.

Many physical and chemical processes occur at the boundary between two phases, while others are initiated at that interface. An understanding of phenomena occuring at such boundary surfaces is therefore often assential for explaining the mechanism of, for example, dissolution and crystallization.

Adsorption is one of the fundamental surface phenomena (as well as a unit operation). However, atoms on the surface of the adsorbent are not totally surrounded by other adsorbent atoms and therefore can attract adsorbates. The exact nature of the bonding depends on the details of the species involved, but the adsorption process is generally classified as physisorption (characteristic of weak van der Waals forces) or chemisorption (characteristic of covalent bonding) (Fig. 2.17).

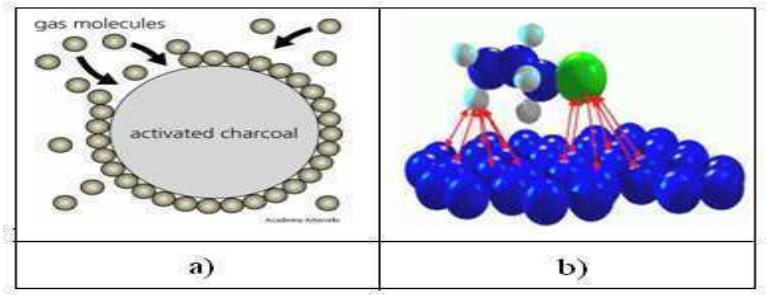

Figure 2.17 a) Physisorption, b) Chemisorption (Kaplan, 2009).

Adsorption can take place at the following interfaces the process of adsorption in the following system (Oscik, 1982):

1. liquid/gas, 2. solid/gas, 3. solid/liquid, 4. liquid/liquid

The necessary condition for adsorption is that one of the phases must be a fluid in which the adsorbate can diffuse freely.

2.3.2 Adsorption isotherms

Adsorption is usually described through isotherms, that is, the amount of adsorbate adhering on the adsorbent as a function of its pressure (if gas) or concentration (if liquid) at constant temperature. The quantity adsorbed is nearly always normalized by the mass of the adsorbent to allow comparison of different materials.

Langmuir adsorption isotherm

In 1916, Irving Langmuir published a new model isotherm for gases adsorbed on solids, which retained his name. It is a semi-empirical isotherm

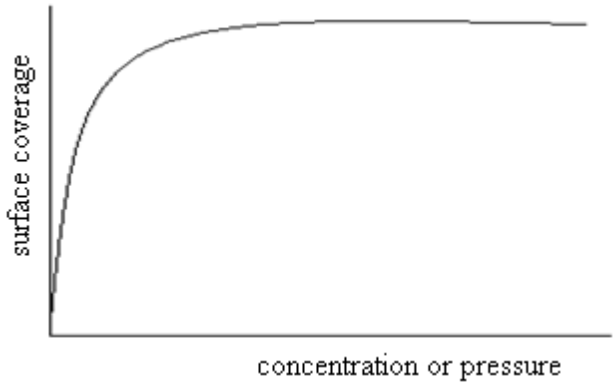

Figure 2.18 Langmuir's adsorption isotherm

. derived from a proposed kinetic mechanism. It is based on four assumptions:

1. The surface of the adsorbent is uniform, that is, all the adsorption sites are equivalent.

2. Adsorbed molecules do not interact.

3. All adsorption occurs through the same mechanism.

4. At the maximum adsorption, only a monolayer is formed: molecules of adsorbate do not deposit on other, already adsorbed, molecules of adsorbate, but only on the free surface of the adsorbent.

The Langmuir equation or Langmuir isotherm or Langmuir adsorption equation relates the coverage or fraction of surface on which molecular adsorbed on a solid surface to gas partial pressure or concentration of a medium above the solid surface at a fixed temperature. The equation was developed by Irving Langmuir in 1916. The equation is stated as:

$$\theta = \frac{\alpha * P}{1 + \alpha * P} \tag{2.18}$$

θ or theta is the fractional coverage of the surface, P is the gas partial pressure or concentration, α alpha is a constant. The constant α is the Langmuir adsorption constant and increases with an increase in the binding energy of adsorption and with a decrease in temperature.

The Langmuir equation is expressed here as:

$$\Gamma = \Gamma_{max} * \frac{Kc}{1 + Kc} \tag{2.19}$$

where K = Langmuir equilibrium constant, c = aqueous concentration (or gaseous partial pressure), Γ = amount adsorbed, and Γ_{max} = maximum amount that can be adsorbed as c increases.

The reciprocal of the Langmuir equation yields the Lineweaver-Burk equation:

$$\frac{1}{\Gamma} = \frac{1}{\Gamma_{max}} + \frac{1}{\Gamma_{max} Kc} \tag{2.20}$$

A plot of (1/Γ) versus (1/c) yields a slope = $1/(\Gamma_{max}K)$ and an intercept = $1/\Gamma_{max}$.

BET adsorption isotherm

Often molecules do form multilayers, that is, some are adsorbed on already adsorbed molecules and the Langmuir isotherm is not valid (Fig. 2. 19).

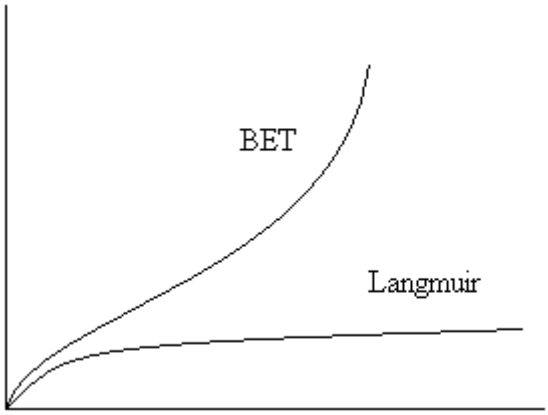

Figure 2.19 BET's adsorption isotherms.

In 1938 Stephan Brunauer, Paul Emmett, and Edward Teller developed a model isotherm that takes this possibility into account. Their theory is called BET theory, after the initials of their last names. The derivation of the formula is more complicated than Langmuir's.

The Langmuir equation is expressed here as:

$$\frac{x}{v(1-x)} = \frac{1}{v_{mon}c} + \frac{x(c-1)}{v_{mon}c} \qquad (2.21)$$

x is the pressure divided by the vapor pressure for the adsorbate at that temperature (usually denoted P / P^0), v is the STP volume of adsorbed adsorbate, v_{mon} is the STP volume of the amount of adsorbate required to form a monolayer and c is the equilibrium constant *K* we used in Langmuir isotherm multiplied by the vapor pressure of the adsorbate. The key assumption used in deriving the BET equation that the successive heats of adsorption for all layers except the first are equal to the heat of condensation of the adsorbate.

The Langmuir isotherm is usually better for chemisorption and the BET isotherm works better for physisorption for non-microporous surfaces.

Freundlich's adsorption isotherm

Boedecker proposed in 1895 an emprical equation for the adsorption in the form:

$$a = k\, p^{1/n} \tag{2.22}$$

where k and n are constants. This equation is known as Freundlich's adsorption isotherm equation, because Freundlich assigned great importance to it and popularized its use. It has been widely used as an empirical equation for qualitative purposes, and seemed to have no particular theoretical foundation.

Kisliuk adsorption isotherm

Molecular interactions between gas molecules adsorbed on a solid surface form significant interactions with gas molecules in the gaseous phase. Hence, adsorption of gas molecules to the surface is more likely to occur around gas molecules that are already present on the solid surface, rendering the Langmuir adsorption isotherm ineffective for the purposes of modelling. This effect was studied in a system where nitrogen was the adsorbate and tungsten was the adsorbent by Paul Kisliuk in 1957.

$$\theta_{(t)} = \frac{1 - e^{-R'(1+k_E)t}}{1 + k_E e^{-R'(1+k_E)t}} \tag{2.23}$$

k_E : Sticking coefficient.

R' : The rate constant for the Kisliuk model.

$\theta_{(t)}$: Fractional coverage of the adsorbent with adsorbate.

t : Immersion time.

2.3.3. Adsorption on metal oxide surfaces

Since the surface of metal oxides is usually covered with chemisorbed water, i.e., surface hydroxyls, its adsorptive behavior and catalytic action should be affected by the presence of surface hydroxyls. The knowledge of the numbers

of surface hydroxyls, therefore, is necessary for the critical discussion of the interaction between metal oxide surfaces and adsorbate molecules (Nagao and Morimoto, 1980).

Hydroxyl species on metal oxide surfaces have received considerable attention in recent years, because their presence has pronounced effects on the chemical activity and electronic properties of oxide surfaces (Noei et al., 2008).

2.3.4 Adsorption of surfactants

Surfactant adsorption is widely used to achive changes is wetting, colloidal properties, and lubrication. Many surfactant are charged, and it is well-known that the charge on the solid-liquid interface affects the amount of adsorption, the shape of the adsorption isotherm, and the organization of the adsorbed surfactant molecules (Tulpar and Ducker, 2003).

Some aspects of surfactant adsorption to solid surfaces are clear. For example, charged surfactants adsorb readily by electrostatic interactions on oppositely charged surfaces. A characteristic feature of surfactant adsorption at concentrations below the critical micelle concentration (cmc) is that adsorbed surfactants form local aggregates (Hu and Bard, 1997).

Sodium dodecyl sulfate is known to hydrolyze over time to form dodecanol which enhances the adsorption of SDS below the critical micelle concentration (cmc) (8.1mM) and decreases the adsorbed amount above the cmc. The dodecanol impurity can exist in commercially available SDS purity on SDS adsorption equilibria. A decrease in the adsorbed amount of surfactant above the cmc can be associated with solubilization of dodecanol in SDS micelles in the bulk (Levchenko et al., 2002).

2.3.5 Instruments used in measuring adsorption behavior

Adsorption has been intensively investigated with experimental techniques, such as scanning tunneling microscopy (STM), low-energy electron diffraction (LEED), x-ray diffraction, Raman spectroscopy, small-angle x-ray spectroscopy (SAXS), nuclear magnetic resonance (NMR), temperature-programmed desorption (TPD), and many others. These methods provide detailed information about physicochemical properties of solid surfaces and adsorbates.

3. EXPERIMENTAL

3.1 Materials and methods

3.1.1 Materials

(SDS) Sodium Dodecyl Sulfate: SDS is used as the surfactant to be adsorbed in this work. It is an anionic surfactant and has molecular formula of $C_{12}H_{25}OSO_3Na$. SDS has a purity of greater than 99.00% (FLUKA). Its molecular weight is 288.38 g/mol. It is used without further purification. 1-16mM of its solutions are used in all the experiments. The solutions are prepared by weight determined g SDS in a 250 mL volumetric flask and filling the flask up to 250 mL with distilled water. SDS solutions are placed into ultrasonic water bath for 15minutes and they are mixed by IKA-Labortechnik RH basic magnetic stirrer for 20minutes. Finally, solutions are kept in cooled incubator at 25^{o}C.

(ZnO) Zinc Oxide: Zinc oxide has a purity of 99% (MERCK). Its molecular weight is 81.39 g/mol. This material has a medium particle size of 530 nm and a BET surface area of 5.17 m^2/g. Before experiments, ZnO was dried at 250^{o}C for 5hours. 1g of ZnO is used in all adsorption experiments.

Water: Distilled water with a conductivity and pH value of 1.7 μS/cm and 5.58, respectively, in all experiments.

(NaOH) Sodium Hydroxide: Sodium Hydroxide pellets purity 99.9% (MERCK) is used in the experiments. Its molecular weight is 40 g/mol. It is used without further purification. 0.01 M and 0.1 M of its solutions are used in all the experiments. The solutions are prepared by weighing 0.4 g and 4 g of sodium hydroxide in a 1 L volumetic flask and filling up to 1 L with distilled water.

(HCL) Hydrochloric Acid: An aqueous hydrochloric acid solution from J.T. BAKER consisting of 36-38% hydrochloric acid is used without further purification. The density of hydrochloric acid is 1.19g/mL and its molecular weight is 36.46 g/mol. 0.01 M and 0.1 M of its solutions are used in all the experiments. The HCL solutions are prepared by taking 0.83 mL and 8.3 mL of HCL solutions and filling up to 1 L with distilled water.

(C_2H_5OH) Ethanol: Extra pure ethanol has a purity of 99.5% (Kimetsan). Its molecular weight is 46.07 g/mol and its density is 0.79-0.82 g/cm^3 (20^{o}C).

($C_4H_9COCH_3$) Methyl Isobutyl Ketone(MIBK): Its molecular weight is 100.16 g/mol and its density is 0.80 g/cm^3 and is bought from ATABAY.

Tego trant A100: Solid powder Tego trant A100 is titrant for the determination of anionic surfactants and soaps (METROHM).

Tego add: Liquid Tego add is solubilizer for the determination of ionic surfactants(METROHM).

Glassware: Before every experiment, all glassware were cleaned with tap water and repeatedly washed with distilled water followed by drying at 70 ^{o}C for 24 h.

3.1.2 Methods

The ZnO is dried by CARBOLITE FURNACES HTC 1400 sinter furnace at 250-300 ^{o}C for 5 h. In the adsorption and desorption experiments the solid suspensions were mixed in NUVE ST 402 shaker water bath for 24 hours. The surfactant concentration is determined by METROHM 785-DMP Titrino with Surfactrode Resistant electrode. The solid ZnO and liquid phases are separated in HETTICH EBA-21 centrifuge at 5000 rpm for 15 min. The required amounts of species are wieghted by using the Sartorius GP603-S scale and all the samples are kept at 25^{o}C in a NUVE ES500 incubator. The samples and species are mixed by IKA-Labortechnik RHbasic magnetic stirrer and also with IKA-Werke mechanical stirrer. The suspensions are stabilized in ELMA Ultrasonic LC30 sonicator. The all glassware are dried in NUVE KD 200 drying oven at 60-70^{o}C for 24 hours. pH and conductivity measurements are performed with a WTW PH 330/SET-1 and WTW COND 340i /SET, respectively. The dried samples are kept in a silica gel-desicator at constant low humidity. Surface charge density of ZnO is determined with potentiometric titration method. Crystal Structure of ZnO is determined with Phillips X'Pert Pro X-Ray Diffractometer (XRD) at a scanning rate of 4 deg/min in a 2θ range from 0^o to 80^0, at IYTE MAM. BET surface area of ZnO which was dried at 105^{o}C for 3h was determined with Micromeritics Gemini V, IYTE MAM and Quantachrome-Nova2200, D. E. U Department of Material and Metallurgical Engineering. Images obtained in Scanning Electron Microscopy (SEM) were used to observe the particle shape of materials. Their

surface concentrations (Zn, S, Na, O, N, Si) were made with Energy Dispersive Spectrometer (EDS) analyses working in coordination with SEM, JEOL JSM-6060, D.E.U. The solubility measurement of ZnO at different pH and zinc content of phases is determined by VARIAN spectra atomic absorption spectrophotometer (AAS).

3.2 Simulation and Characterization of ZnO

Prior to adsorption studies, Merck's ZnO powder was characterized by several methods. Crystal structure, particle shape, surface impurities, surface charge and specific surface area of ZnO were determined by XRD, SEM, EDS, potentiometric titration and BET analyses, respectively.

3.3 Charge Regulation of ZnO and Adsorption Conditions

The surface charge of ZnO is depend on pH. This charge is due to surface species $M\text{-}OH_2^+$ and $M\text{-}O^-$ described in section 2.2.2. pH adjustment of the surface species and adsorption were started at same time, large deviation in adsorbed species were observed. When the surface charge was regulated at the given pH and then adsorption started the results were smoother. Thus, surface was convert to stable state with this work.

For charge regulation of ZnO surfaces, 1g ZnO weighed is placed into 50mL volumetric flask and 15mL water at constant pH is poured onto ZnO weighed. Then, this mixture is placed into sonicator for 120 min. Afterwards, 15mL SDS solution at different concentration and at constant pH is poured onto mixture. In the initial experiments maximum adsorption was obtained when 30 mL SDS solution was used for 1 g ZnO. This ratio is kept constant in this research. Finally, this mixture is placed into shaker and kept for a day. Equilibrium is reached after two days and analyses of the supernatant solutions are made to determine the amount of SDS adsorbed on ZnO particles. If the SDS adsorption is made at a pH level different from that of distilled water, pH of the SDS solutions are adjusted with HCL/NaOH before the experiment. All experiments were carried out at constant temperature of 25^oC.

Equilibrium is reached after two days. Then the solutions are poured into the centrifuge tubes and placed into the centrifuge, it rotated at 5000 rpm for 15 min.

After centrifugation, supernatant solutions are taken with a pasteur pipette and these solutions are kept in glass vessels.

Adsorbed amount of SDS (Γ^*) can be calculated from Eq. 3.1, the difference in concentration before and after adsorption of surfactant, ΔC, in a solution of known volume, V, after adsorption equilibrium has been reached, i.e.:

$$\Gamma^* = \frac{\Delta C \text{ x } V}{m} = \frac{\text{mol}}{\text{g ZnO}} \qquad (3.1)$$

where m is the mass of adsorbent.

3.4 Desorption Condition

To see if SDS was adsorbed physically or chemically onto ZnO surfaces, desorption was carried under the same conditions as adsorption. ZnO particles that had adsorbed the SDS at a certain pH were used in the experiments to desorb into the solution under the same conditions. SDS concentration was $9x10^{-3}$M and distilled water was used at different pH values. This SDS solution at $9x10^{-3}$M was adjusted to pH 4, pH 8, pH 10 and pH 12. In addition, SDS solution was used at natural pH. All experiments were carried out at 25^{o}C temperature.

Before the dsorption, solid which was obtained from SDS adsorption at the predetermined pH value was dried at 60^{o}C for 24 h. 30 mL double distilled water was prepared at same pH as the adsorption condition was poured onto this solid. Then, the mixture is placed into the sonicator for 2 hours as in adsorption conditions. Afterwards, this mixture was placed into shaker for a day. Finally, desorbed amount of SDS was determined with titromat.

3.5 Conductivity Measurement

The solutions that were prepared at different SDS concentrations and same or different pH are mixed with magnetic stirrer for 15 minutes. Then, conductivity of solutions were measured with a WTW Cond 340i /SET after all operations are finished.

The critical micelle concentration (CMC) of SDS were determined from conductivity measurements. CMC of SDS is obtained from inflection point on the

the chart, when conductivity is drawn as a function of SDS concentration at different pH values.

3.6 Potentiometric Titration

Surface charge density of ZnO with a surface area of 5.17 m^2/g in aqueous solution of NaCl was determined by potentiometric titration. Titration is performed with four different electrolyte concentrations, 0.001 M, 0.01 M, 0.1 M and 0.5 M NaCl.

Two runs were carried out:

1) 0.1 g ZnO is dispersed in 150 mL electrolyte solution. The initial pH of the system is adjusted to ~ 11 with 0.1 M NaOH. A 0.01 M solution of HCl is used as a titrant in the pH range from 11 to 4. A dose of titrant 0.2 mL/min is added to the system with an automatic titrator (Metrohm 785 DMP Titrino). During the titration, system is stirred with a magnetic stirrer and the pH of the system is measured with a glass pH electrode. Experiments are carried out at 25 ^oC.

2) Blank titration (electrolyte in the absence of ZnO) is performed under the conditions described above.

The difference in acid or base quantities, used to obtain the same pH in solutions with ZnO and the blank, is taken to represent the association or dissociation of H^+ ions from ZnO surfaces.

For this end, ZnO is dispersed in the electrolyte and the initial pH of the medium is adjusted to ~11 with NaOH solution. Experiments are performed by slow addition of titrant -HCl solution- to the dispersion. In each addition of titrant, pH of the medium is measured. Then, Titrant Volume versus pH data are drawn on the chart.

3.7 Solubility of Merck's ZnO

Solubility of Zn^{++} ions are determined as a function of pH, before starting the adsorption experiments at different pH.

The experimental procedure is as follows: The aqueous solution with pH varying between pH=2 and pH=3 are poured on to 1 g ZnO powder. Then, these solutions are mixed with a mechanical stirrer for 10 min. On completion of the mixing, phase separation is observed below the suspended solid ZnO and supernatant solution. When separation is completed, these suspension are filtered with filter paper under the vacuum in order to obtain the solution phase. Finally, the aqueous phase is analyzed with Atomic Absorption Spectrophotometer (AAS), for the Zn^{++} content.

Standard solutions are prepared at different concentrations of Zn^{++} from Zinc acetate dihydrate salt for calibration of the AAS.

3.8 Determination of Stable Regions

When ZnO is immersed into water, several species are formed on ZnO surfaces. These species are important for the surface charge density measurement and adsorption because, they are affected by the variation of pH. As a consequence, experiments were carried out with a 2.9 vol% zinc oxide (2 g), and aqueous solution (12.5 mL) with dilute solutions of HCL and NaOH used to preset the initial pH. The initial pH was monitored as a function of time with the suspension mixed continuously for 4 days.

3.9 BET-Specific Surface Area Analysis

Adsorption of SDS onto ZnO can be determined with this method, also. In this set of experiment, SDS was adsorbed onto ZnO at different concentrations, at natural pH and constant temperature ($25^{o}C$). Concentrations of SDS solutions were between $1x10^{-3}$ M and $16x10^{-3}$ M. Equilibrium was reached after two days. The suspension are poured into centrifuge tubes and it centrifuged at 5000 rpm for 15 min. After the centrifugation, supernatant solutions were taken with pasteur pipettes and kept in glass vessels. The lower phase, obtained after SDS adsorption, were dried at $60^{o}C$ for 24h before determination of the surface area.

BET surface area of ZnO particles are determined by N_2 adsorption-desorption isotherms. Before measurement, samples were dried at 150 ^{o}C for a day.

The results of the BET surface area determinations were used to check the fractional surface coverage of SDS on ZnO by Eq. 3.2.

Fractional surface coverage:

$$\frac{0.57\text{x}10^{-18}\,\frac{\text{m}^{2}}{\text{molecule}}\ \text{x}\ \Gamma^{*}\,\frac{\text{mol}}{\text{g ZnO}}\ \text{x}\ 6.02\text{x}10^{23}\ \frac{\text{molecule}}{1\text{mol SDS}}}{\text{Specific surface area (BET)}\ \frac{\text{m}^2}{\text{g}}} = \frac{1}{\text{m}^2} \qquad (3.2)$$

where 0.57nm^2 is area which is coveraged by a SDS molecule on ZnO surface. Γ^* is adsorbed amount of SDS onto 1 g ZnO.

3.10 SEM and EDS analysis

Images obtained in SEM were used to observe the particle shape of materials. Their surface concentrations (Zn, S, Na, O, N, Si) were determined with EDS (Energy Dispersive Spectrometer) analyses working in coordination with SEM. In this experiment, four samples were analysed with SEM and EDS. $6\text{x}10^{-3}$ M, $8.3\text{x}10^{-3}$ M, $10\text{x}10^{-3}$ M and absence of any SDS molecule in solutions were used at adsorbed medium. After SDS adsorption, the equilibrium was reached after two days solutions that include ZnO particle were deposited on a carbon band and allowing the evaporation of the water at room temperature. The carbon bands, which are deposited with samples, are coated with Au/Pd mixture and are placed under vacuum for 45 minutes. Then, the SEM analyses are performed for different scales. For each sample, elemental analyses are performed with the energy dispersive spectrometer, EDS to be sure of the existence of zinc ions in the system.

3.11 XRD Analysis

The ZnO, Merck ZnO powder that was used for simulation was dried at 250 ^{o}C for 5 h before it was analysed with x-ray diffractometer (XRD). To determine crystal structure of ZnO, X-Ray Diffractometer (XRD) was used at a scanning rate of 4 deg/min in a 2θ range from 0^{o} to 80^{0}.

3.12 Determination of SDS Concentration

Anionic surfactant analysis was made as aforementioned using Automatic Titrator System combined with ‘‘Surfactrode Resistant’’ electrode and 785DMP Titrino (Fig. 3.1).

Figure 3.1 Metrohm 785 DMP titrino.

Potentiometric two-phase surfactant titration is known as the most accurate, precise and quick method and also inexpensive with respect to the spectroscopic analysis methods. The basis of potentiometric surfactant titration is a precipitation titration, in which the analyte is precipitated out with the titrant. The titration produces the optimal S-shaped titration curves (Fig. 3.2).

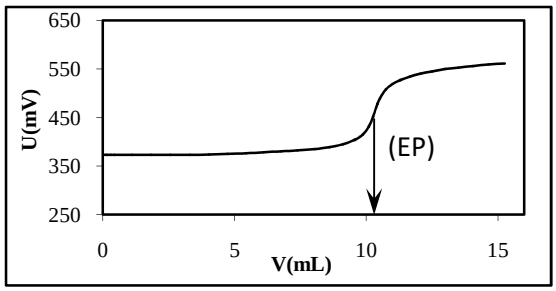

Figure 3.2 S shaped titration curve and determination of end point (EP).

Cationic analytes are titrated with anionic titrants, anionic analytes with cationic titrants. Both titrations can be carried out in the dynamic mode, in which the added volume increments are calculated by a microprocessor according to the change in the electrode potential and then added.

In addition to the automatic titrator system, TEGOTrant A100 (1,3-didecyl-2-methylimidazolium chloride), the cationic surfactant, is used as the ‘‘titrant’’ for anionic surfactant analysis. This titrant possesses a high reaction speed and has a high affinity to the analyte surfactant. The titrant produces larger potential differences between the start of the titration and its end, the largest potential changes occuring in the region of the equivalence point (EP). In this method, the ion associate formed by the analyte and titrant is extracted into the second, organic phase in the titration with the surfactrode resistant as indicator (see Fig. 3.3).

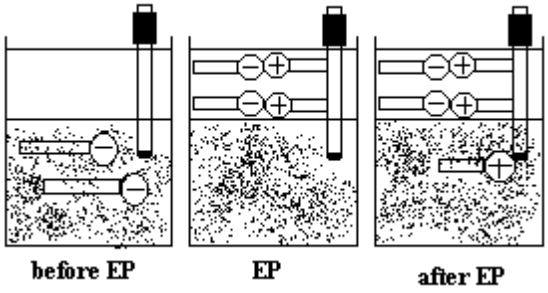

Figure 3.3 Detection principle of two-phase surfactant titration using the metrosensor Surfactrode Resistant.

Titration can be carried out in the presence of a solvent. The addition of solvent immiscible with water is an absolute necessity. The solvent is highly important for the detection. Methyl isobutyl ketone (MIBK) and ethanol mixture is used as our solvent mixture in the anionic surfactant analysis.

Measurement with surfactrode resistant electrode

An example for the determination of SDS concentration is given below: 10 mL SDS solution at $4x10^{-3}$M concentration, 70 mL distilled water and 0.2 mL Tego add are put into a 150 mL glass beaker. Then, the pH of the solution is adjusted to 3.0 with HCL at 0.5 mol/L, with a 1 mL syringe. Then, 20 mL solvent mixture (MIBK and ethanol) is added to the solution with adjusted pH. Afterwards, reference electrode (Fig. 3.4) is taken out of its pot.

Figure 3.4 Reference electrode. Inner and outer fillings are filled with 3M KCL for anionic surfactant analysis.

Reference electrode, surfactrode resistant (Fig. 3.5) and Tego trant A100 transmitter is put to the mechanism. Before dipping this mechanism into the solution, it is mixed until turbity is observed.

Figure 3.5 Surfactrode resistant electrode to analyze the anionic surfactants.

In order to start the titration, we should press the ‘‘start’’ key on the 785 DMP titrino keybord (Fig. 3.1).

Concentration of SDS in solution is calculated from formula given below:

$$C_{Tegotrant} * V_{Tegotrant\ (EP)} = C_{Sample} * V_{Sample}$$

$C_{Tegotrant}$ = Concentration of Tegotrant, (mol/L).

$V_{Tegotrant}$ = Volume of Tegotrant used in experiment during measurement, (mL).

C_{Sample} = Concentration of sample, (mol/L).

V_{sample} = Volume of sample used in experiment during measurement, (mL).

4. RESULTS AND DISCUSSION

4.1 Simulation and Characterization of Merck's ZnO

A series of tests were conducted to see if the ZnO particles produced by Merck could be used to simulate the ZnO nanoparticles produced in the Project 104 M 382.

4.1.1 XRD analysis

Characterization of the particles were started with XRD analysis to determine the crystal structure of ZnO (Fig. 4.1).

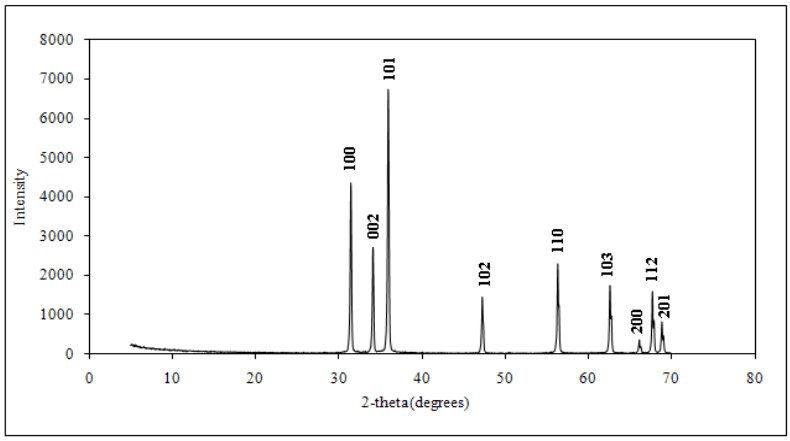

Figure 4.1 Wurtzite crystal structure of Merck ZnO.

As seen Fig. 4.1, XRD analysis of Merck's ZnO showed similar result with both ZnO produced in the Project and literature; e.g., wurtzite crystal structure.

4.1.2 SEM and EDS analysis

As a second characterization, SEM and EDS analysis of Merck's ZnO were made with Scanning Electron Microscopy (SEM) and Energy Dispersive Spectrometer (EDS), respectively. As seen Fig. 4.2, SEM images of Merck's ZnO showed that the particles were short cylinders with hexagonal cross-sections. In particular, shape of ZnO particles in circle on the right-hand of SEM Picture have hexagonal cross sections.

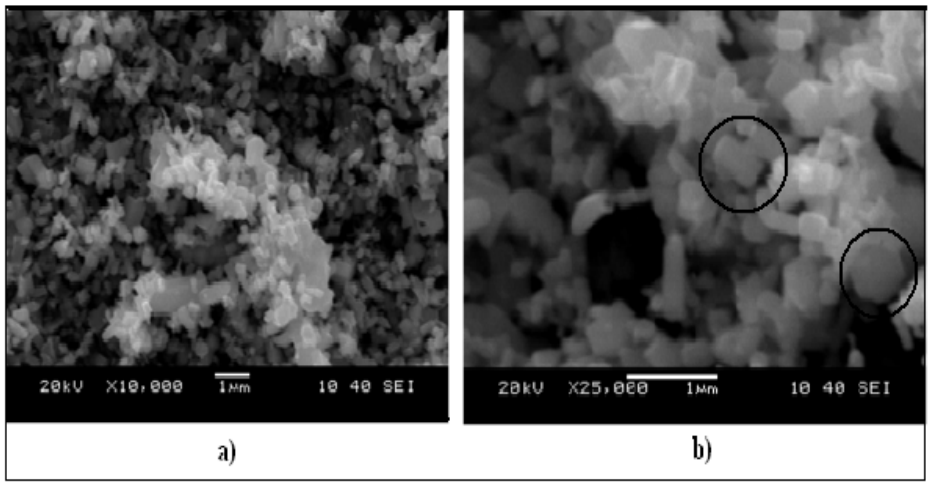

Figure 4.2 SEM images of Merck' ZnO.

Their dimensions were in the order of nanometers. So, we decided Merck ZnO were similar in size in with in the same order of dimensions magnitude as the nanoparticles produced in the Project.

In addition, surface composition of Merck's ZnO was analysed with EDS analysis (Fig. 4.3).

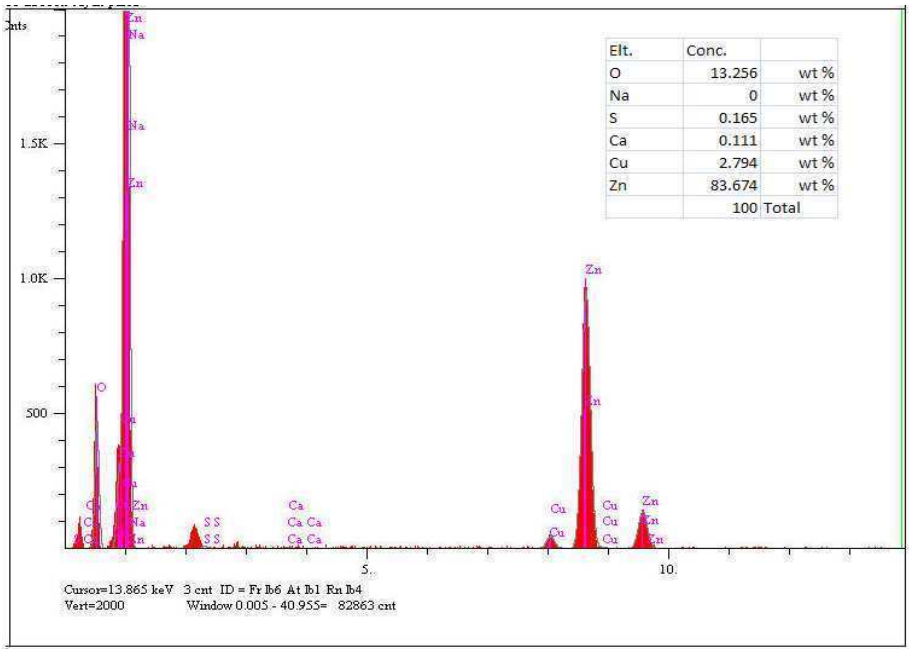

Figure 4.3 EDS analysis of Merck's ZnO.

The results showed the presence of sulphur at surfaces of Merck's ZnO, also. In this case, there were sulphur ions and some impurities that could not be removed on the Merck's ZnO surfaces during fabrication of ZnO.

4.1.3 BET-Specific surface area analysis

BET surface areas of commercial ZnO was found as 5.17 m^2/g. From this data, surface area of Merck's ZnO was smaller than that of products produced in the project (BET : 40.35 m^2/g). This was mainly because the surfaces of commercial rods were rather smooth, where in the Project the rods were made up of globuler stick together. So we decided to used commercial ZnO as simulation material.

4.1.4 Surface Charge Density Measurement

Surface charge density of Merck's ZnO was obtained by potentiometric titration method at different electrolyte (NaCL) concentration (Fig. 4.4).

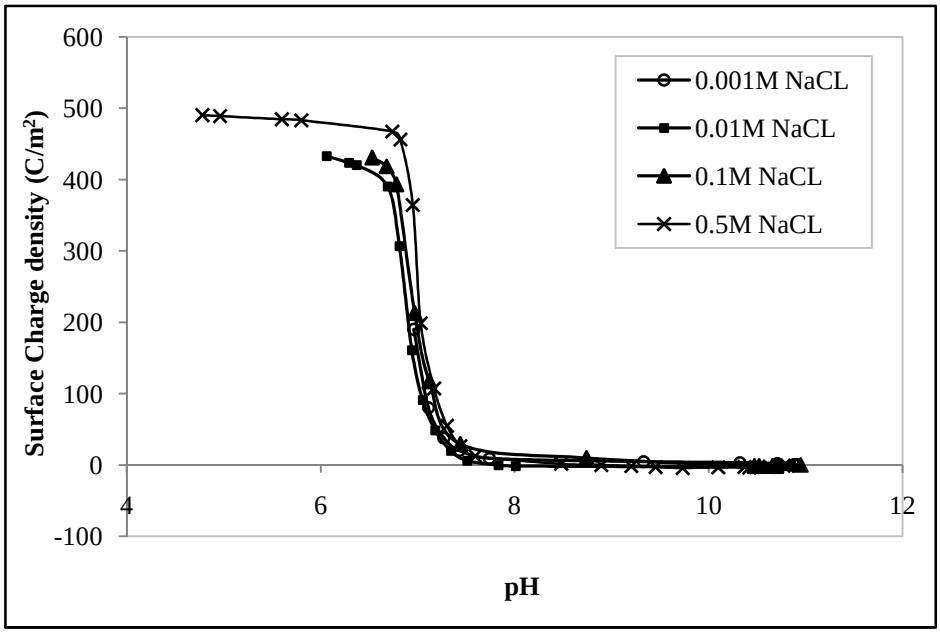

Figure 4.4 Surface charge density measurement of Merck's ZnO.

As seen Fig. 4.4, surface charge density increases with increasing electrolyte concentration of dispersion solution. Due to amphoteric properties of ZnO, surface charge density of ZnO between pH 6.8 and 7.8 increases perceptibly. In this region, neutralization takes place by titration of the base with acid. Surface

charge transforms to pozitive values completely and becomes stable. The most time is spent in here during potentiometric titration experiment by device. At lefthand and righthand of this S-shape, surface charge density changes easly, but variation of surface charge density is little. Between pH 8 and pH 11, surface is covered with OH^- ions and at pH<6.8, surface covered with H^+ ions. The slope of S-shape becomes a most horizontal with decrease in electrolyte concentration.

In addition, point of zero charge (pzc) of merck's ZnO was affected by the concentration of electrolyte. As given in Fig. 4.5, pzc value of ZnO decreases with increase of electrolyte concentration.

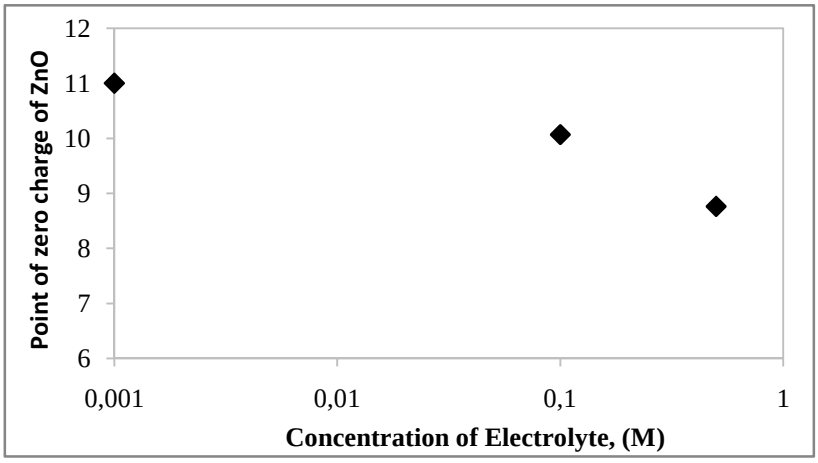

Figure 4.5 Variation of pzc with concentration of electrolyte.

To adjust the pH of electrolyte solution during experimenal, 1 mL, 1.5 mL and 3mL NaOH solutions were used to fix the pH of 0.001 M, 0.1 M and 0.5 M electrolyte concentration, respectively. So, pzc of ZnO decreases with increasing concentration of OH^- ions in solution, because ZnO surface is covered with OH^- and some species are formed such as $Zn(OH)_{3\,(aq)}^-$ and $Zn(OH)_{4\,(aq)}^{2-}$ (Fig. 2.16) (Eq. 2.6 – Eq. 2.11). The increasing of these species lower the pH of zero charge from pH = 11 and pH = 8.76.

Different values are given in the literature for the range of pH in which pzc is observed that confirm with our results by shaking that the pzc is observed in the interval 6.9 < pH < 9.8, that change as a function of the electrolyte concentration (Sedlak and Janusz).

4.1.5 Solubility of Merck's ZnO

The solubility in terms of mol percent Zn^{++} that passes into the solvent phase is given in Fig. 4.6 as a function of pH (Appendix A, Table A.1). The solubility of Zn^{++} remains approximately constant in the range $1x10^{-2} – 1x10^{-3}$ for the interval 4 < pH < 11.

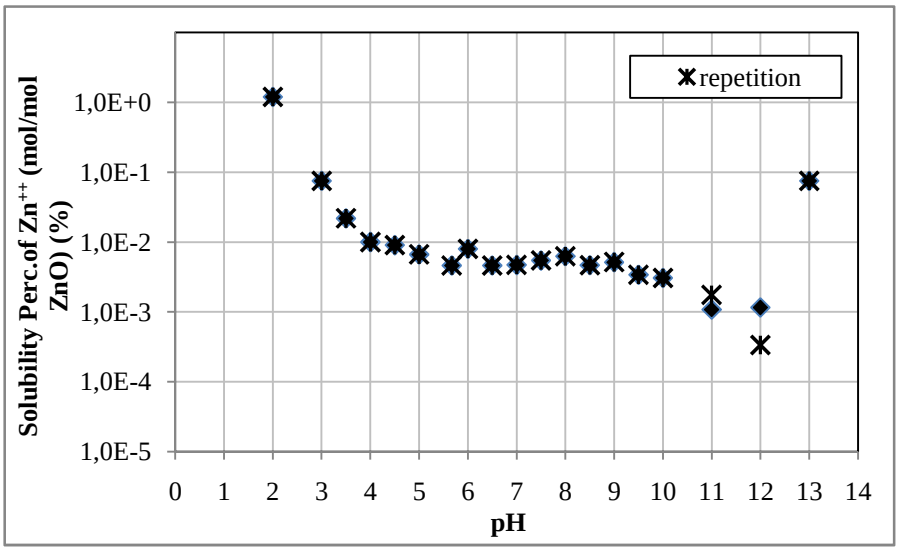

Figure 4.6 Solubility diagram for ZnO.

Solubility percentage of Zn^{++} decreases for pH > 9.5 and reaches a minumum at pH 12. The solubility of Zn^{++} increases again for pH > 12. Accordring to Sedlak and Janusz (2008), the minumum solubility of ZnO is observed in the interval pH = 9.9 < pH < 12.3, because ZnO dissolution takes place according to Eq. 2.6 - 2.16 in aqueous solution.

4.1.6 Determination of Stable Region

In the literature (Degen and Kosec, 2000) it was reported that the pH of the suspension can not be set of certain value, and that the preset value decreased as a function of time due to formation of zinc species on ZnO surfaces. A set of experiments were carried out to see the extent of instability in our system. The experiment was carried out with a 2.9 vol% zinc oxide (2 g) aqueous suspension (12.5 mL) with dilute solutions of HCL and NaOH used to preset the initial pH. The preset values of pH was in the range from 5.12 to 12.3 (Table 4.1). The variation of the preset pH values with time are given in Fig.4.7. Two stable regions were observed where the difference between the initial and final pH: pH < 7.75 and pH > 12.

Table 4.1 Variation of pH with time.

PH_{PRESET}	PH_{FINAL}			
	1.day	**2.day**	**3.day**	**4.day**
5.12	5.23	5.23	5.26	5.26
6.00	5.96	6.06	6.06	6.04
6.99	6.91	6.89	6.88	6.89
8.01	7.99	7.98	7.91	7.87
9.00	8.51	8.50	8.47	8.46
10.00	9.67	9.34	9.19	9.10
11.01	10.43	10.34	10.23	10.14
12.03	11.98	11.99	11.98	11.96

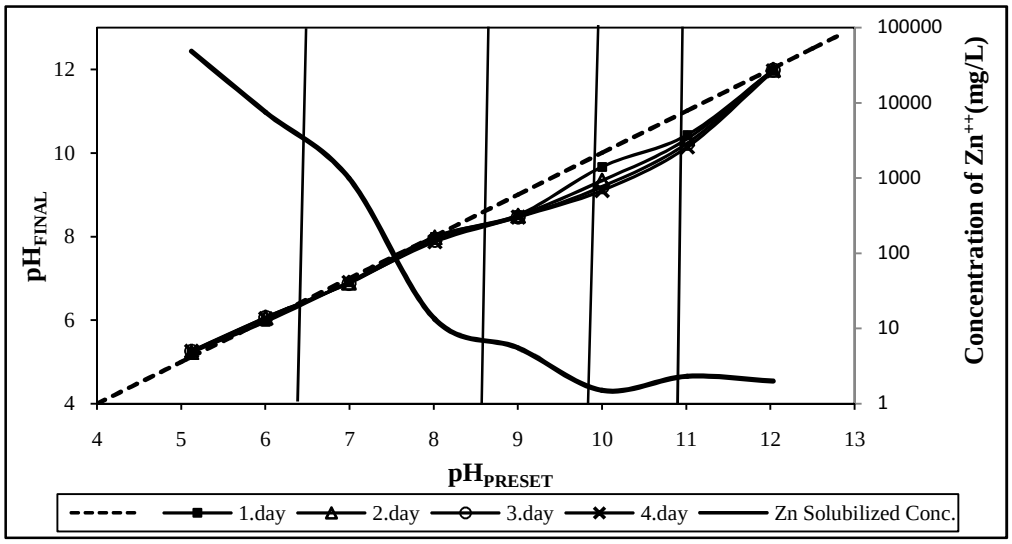

Figure 4.7 Variation of pH with time.

Between these two stable regions, there is a unstable pH region with the greatest variation observed at an initial pH = 10. All experiments carried out in this region showed a decrease of final pH with time. Fig. 4.7 shows that the inherent pH of the zinc oxide suspension at pH = 7.75 is very stable (Appendix B, Table B.1).

The decrease of the final pH with time can be explained by a small dissolution of the zinc oxide or surface hydroxide $Zn(OH)_{2(s)}$ and the formation of different zinc species i.e., $Zn(OH)^{-}_{3(aq)}$ and $Zn(OH)^{2-}_{4(aq)}$. The preset pH =10 of the suspension decreased to 9.1 after 4 days. When the zinc oxide powder was immersed in the water, the surface of the oxide particles was hydrolized because of the physically and chemically adsorbed polar water molecules and a layer of zinc hydroxide is formed. By the addition of the sodium hydroxide solution we preset the pH of the suspension to 10 and the surface hydroxide $Zn(OH)_{2(s)}$

(Eq. 2.8) to the additionally hydrated particles of $Zn(OH)_{2(aq)}$, which is the most stable species at this pH. Colloidal particles of $Zn(OH)_{2(aq)}$ leave the metal oxide surface. Zinc oxide surface is hydrolized again in the reaction of the OH^- ions with the surface zinc atoms. Because of this the concentration of OH^- ions decrease until the final pH = 9.1 is reached after 4 days.

As seen Fig. 2.16, Zn^{++} ions concentration were decreased with an increase of pH and it was minimum at pH 10. This result similar to Fig. 4.7 which is in agreement with the literature results (Degen and Kosec, 2000). From figure 4.7 it can be seen that the minimum solubilization of Zn^{++} is occured between pH 9.8 and pH 12.

We can conclude that the pH of the suspension decreases in the pH region where the $Zn(OH)_{2(aq)}$ particles are present the solution.

4.2 Adsorption

In the Introduction part of this thesis, solvents were found to be unable to dissolve the adsorbed SDS, as given in Table 1.1. This suggested that other interactions were found to strongly affected the adsorption of SDS on the surfaces. These interactions were explained to be due to positive surface charge of ZnO below the point of zero charge, and to be due to surface composition of ZnO corresponding to the pH of the solution determined by solution of ZnO through the reactions given in section 2.2.2.

This adsorption experiments were made in two stage

1. In the first stage, the ZnO particles were immersed into the SDS solution without any adjustment of pH, and the adsorbed amount was determined as a function of SDS concentration.

2. In the second stage, the pH of the solution was adjusted to the preset value, after which it was divided into two portions. ZnO was immersed into one of the portions for preconditioning of the surfaces. All of the SDS was dissolved in the second portion, and the two portions mixed after the surfaces were equilibrated with the blanc solution.

4.2.1 Adsorption without surface conconditioning

4.2.1.1 Determination of adsorbed amount of SDS at natural pH

Initially the weight of solution to ZnO was determined to determine the optimum ratio at which adsorption would be maximized. The maximum adsorption of SDS onto ZnO was obtained for 30 mL SDS solution as given in Fig. 4.8, corresponding to a solution ZnO weight ratio of approximately 30.

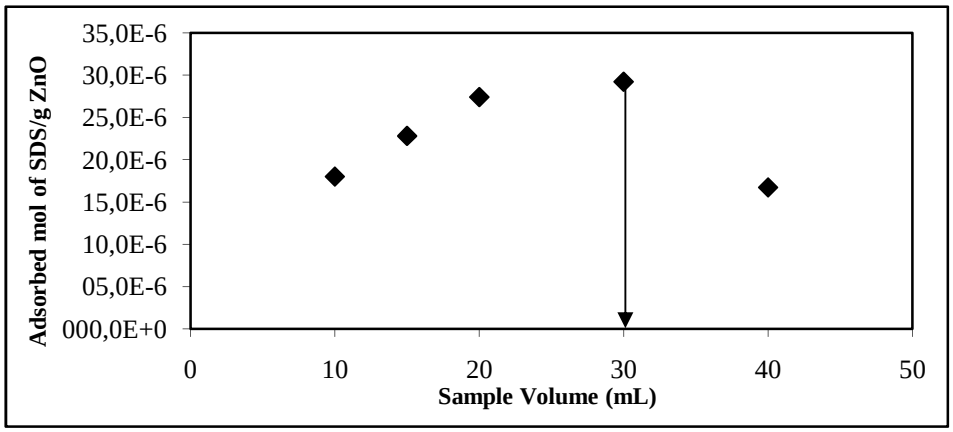

Figure 4.8 Determination of the optimum SDS solution volume to used in the experiments.

According to our experimental results, the isoelectric point of ZnO used in this study changes in the range 8.7 and 11 as a function of electrolyte concentration. At pH 6 (natural), ZnO is positively charged.

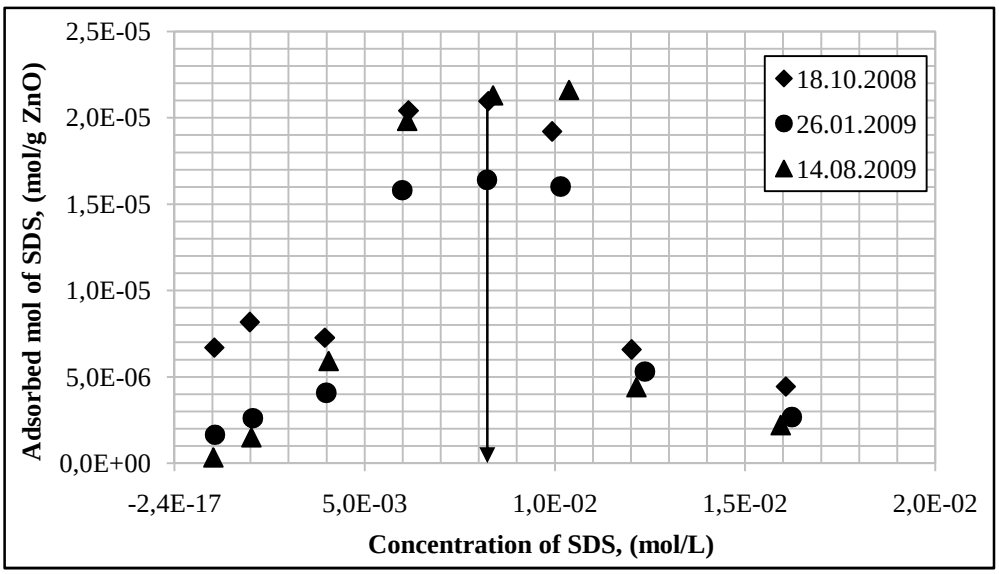

Figure 4.9 Adsorbed amount of SDS, (mol/g ZnO).

Anionic sodium dodecyl sulfate (SDS) by itself can adsorb on ZnO due to electrostatic interaction. At lower surfactant concentrations, SDS adsorption takes place mainly due to electrostatic attraction between the negatively charged dodecyl sulfate and positively charged ZnO (Fig. 4.9).

As can be seen Fig. 4.9, maximum adsorption occurres at CMC ($8.3x10^{-3}$M) value of SDS aqueous solution. Adsorbed amount of SDS can be assumed as constant at $6x10^{-3}M < C_{SDS} < 10x10^{-3}M$. The decrease in the adsorbed amount after $10x10^{-3}$M can be explained by some impurities on surface and dodecanol formation.

According to Levchenko et al., (2002), sodium dodecyl sulfate is known to hydrolize over time to form dodecanol, which enhances the adsorption of SDS below the critical micelle concentration (cmc) (8.3mM) and decreases the adsorbed amount above the cmc. The dodecanol impurity can exist in commercially available SDS if used as received. In addition to this a maximum in the surface excess at a bulk surfactant concentration below the cmc results from the presence of dodecanol in the adsorbed SDS. A decrease in the adsorbed amount of surfactant above the cmc can be associated with solubilization of dodecanol in SDS micelles in the bulk.

The explanation given above seemed logical because polar head group of SDS molecules can be associated with polar molecules such as dodecanol. In addition to the van der Waals forces among the hydrocarbon chains.

As seen Fig. 4.10, At lower concentrations (conc. < $4x10^{-3}$M), both SDS and dodecanol adsorb on the solid surface by themselves due to either electrostatic interaction or hydrogen bonding. At still higher concentrations, intermediate conc., interactions between hydrophobic chains of the surfactants take place leading to a rapid rise in adsorption ($4x10^{-3}$ M< conc. < $8x10^{-3}$M). The mixed aggregates start to form at solid/liquid interface. At high concentration, the most amount of dodecanol molecules can be joined to micelle structure. So, adsorbed amount of SDS can be decreased becasue of repulsion interaction between polar head groups of SDS adsorbed molecules onto ZnO.

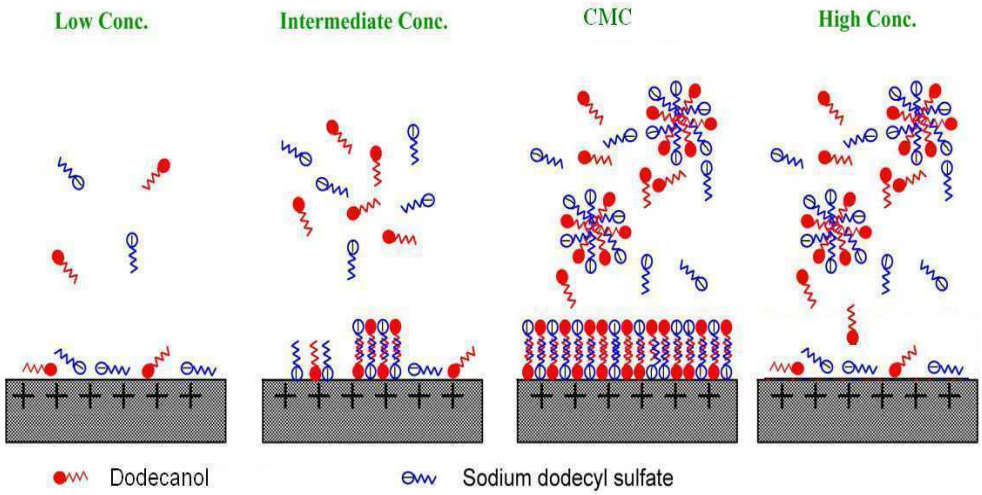

Figure 4.10 Adsorption model for dodecanol/SDS mixtures on the positively charged ZnO.

The Zn^{++} ions in the supernatant solution after the adsorption were determined by atomic adsorption spectrometer. Zn^{++} concentration arises steeply at very low concentrations and remains constant up to about $10x10^{-3}$ M after which it increases slowly (Fig. 4.11). Zeng et al. (2007) showed Zn^{++} ions were adsorbed by micelles, also. This is in confirmation with the adsorption results in Fig. 4.9, coupled with the model sketched in Fig. 4.10. That the initial and final adsorbed amounts in Fig. 4.9 (the dotted line) are approximately the same confirms the model.

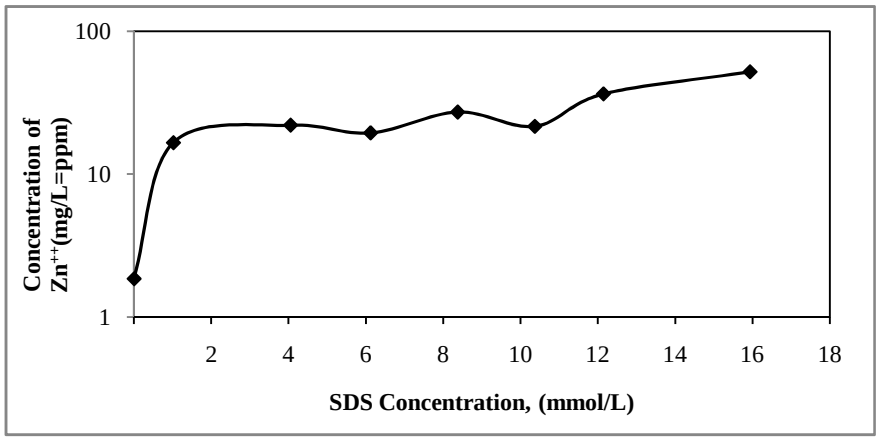

Figure 4.11 Adsorption of Zn^{++} ions by micelles.

The SDS micelles which have negative surface charge adsorbed Zn^{++} ions as seen Fig. 4.12.

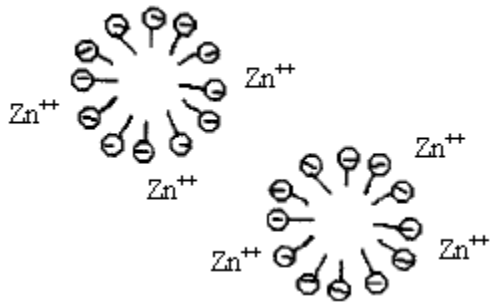

Figure 4.12 Adsorption view of Zn^{++} by micelles.

4.2.1.2 SEM and EDS analysis

From SEM images, SDS adsorption at different concentration was not seen clearly. All images were similar to each other (Fig.4.13).

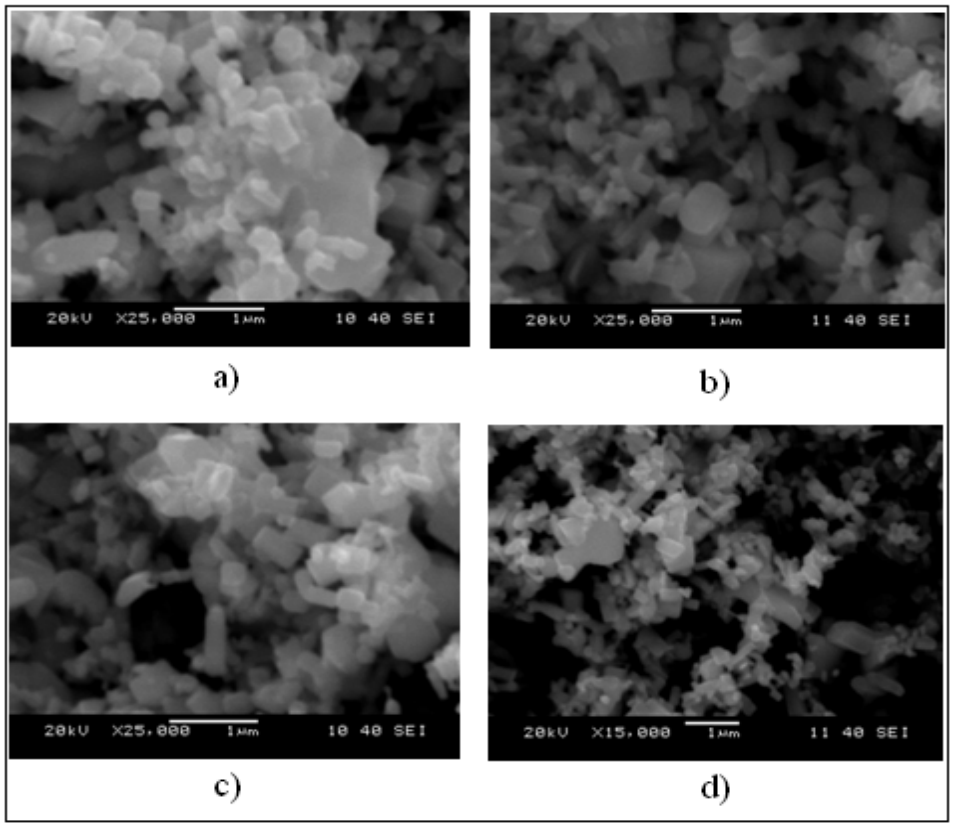

Figure 4.13 SEM images: a) ZnO without SDS, b) $6x10^{-3}$ M SDS, c) $8.3x10^{-3}$ M SDS (cmc), d) $10x10^{-3}$ M SDS.

From EDS analysis results, SDS adsorption can be determined clearly because of amount of sulphur (S) ions on ZnO surfaces.

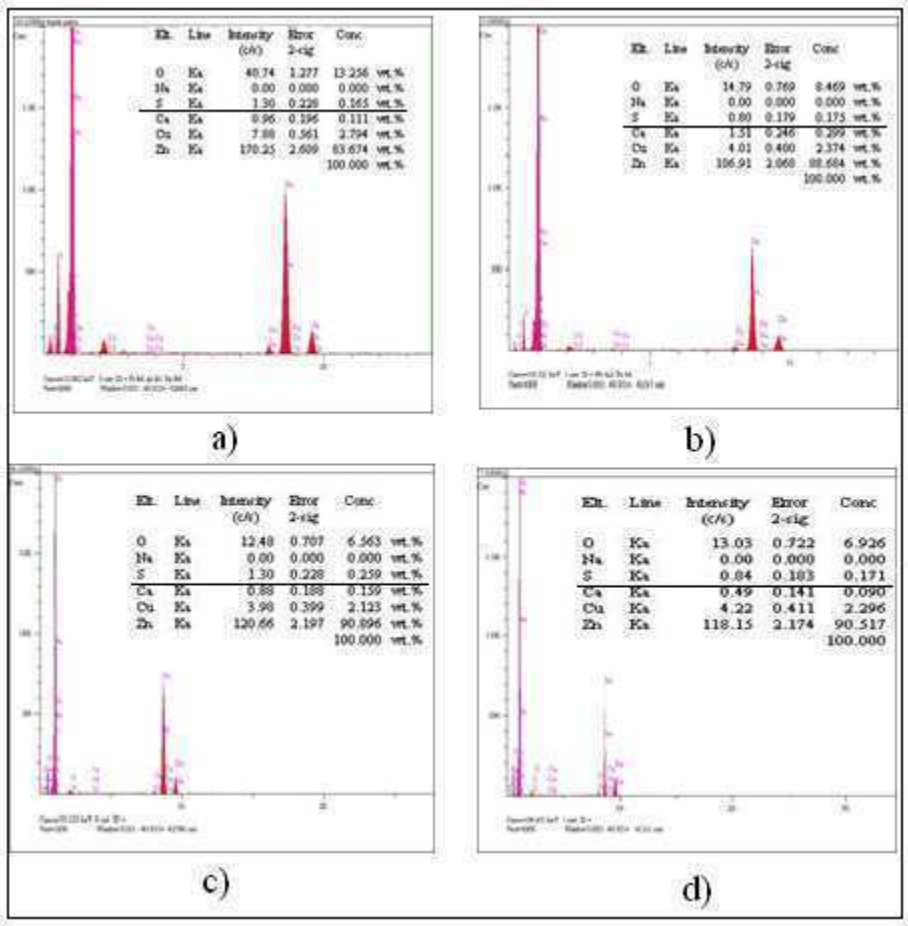

Figure 4.14 EDS analysis: a) ZnO without SDS, b) $6x10^{-3}$M SDS, c) $8.3x10^{-3}$M SDS (cmc), d) $10x10^{-3}$M SDS.

A summary of Fig. 4.14 is given in Table 4.2 in terms of the amount of sulphur and other materials on the surface of ZnO particles.

Table 4.2 Surface composition of ZnO particles as determined by EDS.

Conc. of SDS (mM)	S %W	Na %W	Zn %W	O %W	Ca %W	Cu %W
without SDS	0.165	0	83.674	13.256	0.111	2.794
6	0.175	0	88.684	8.469	0.299	2.374
8.3	0.259	0	90.896	6.563	0.159	2.123
10	0.171	0	90.517	6.926	0.09	2.296

As seen Fig. 4.14 and Table 4.1, the maximum amount of sulfur ions were found at $8.3x10^{-3}$ M , that is, cmc point of SDS molecules. Unfortunately S is present in ZnO particles remaining after production. So, the values in Table 4. 2 are relatived

quantities. Even the relative quantities are in confirmation with the adsorption results.

4.2.1.3 BET analysis

It could be interesting to see the variation of surface area (BET) determined by N_2 adsorption with the adsorbed amount of SDS.

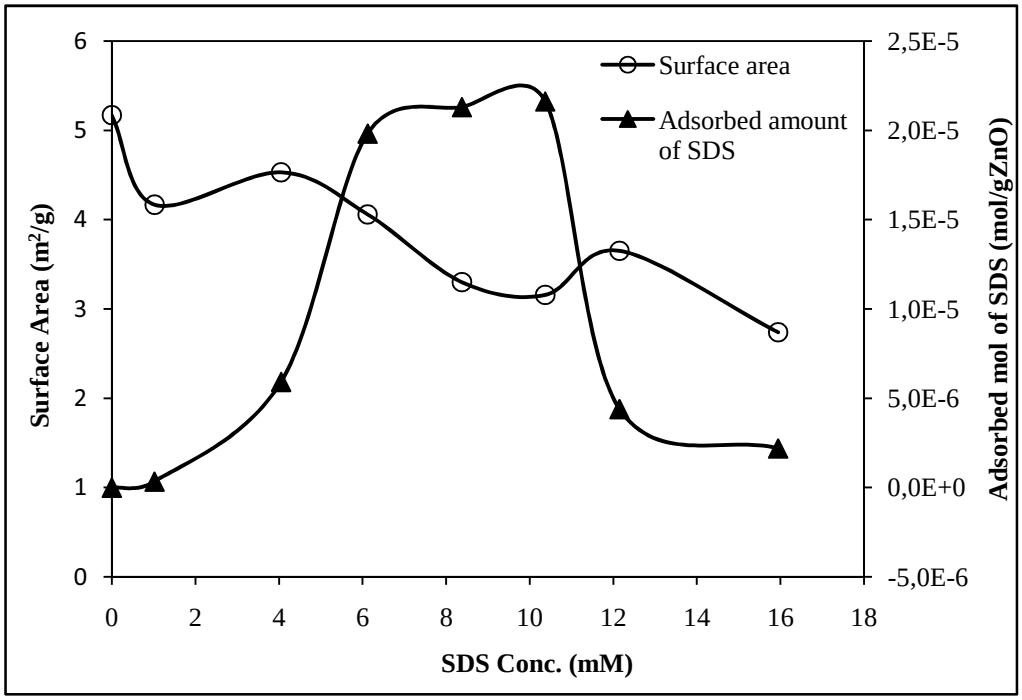

Figure 4.15 BET analysis of ZnO after adsorption.

As given in Fig. 4.15, the surface areas are inversely proportional with adsorbed amount of SDS. İndeed, specific surface area of ZnO has decreased with the increase in the adsorbed amount of SDS onto ZnO. The maximum surface area value was obtained for ZnO without SDS adsorption. In Fig. 4.15, two value, of Surface area (BET) results, 1mM SDS and 16 mM SDS were not right, it can be the experimental error during measurement.

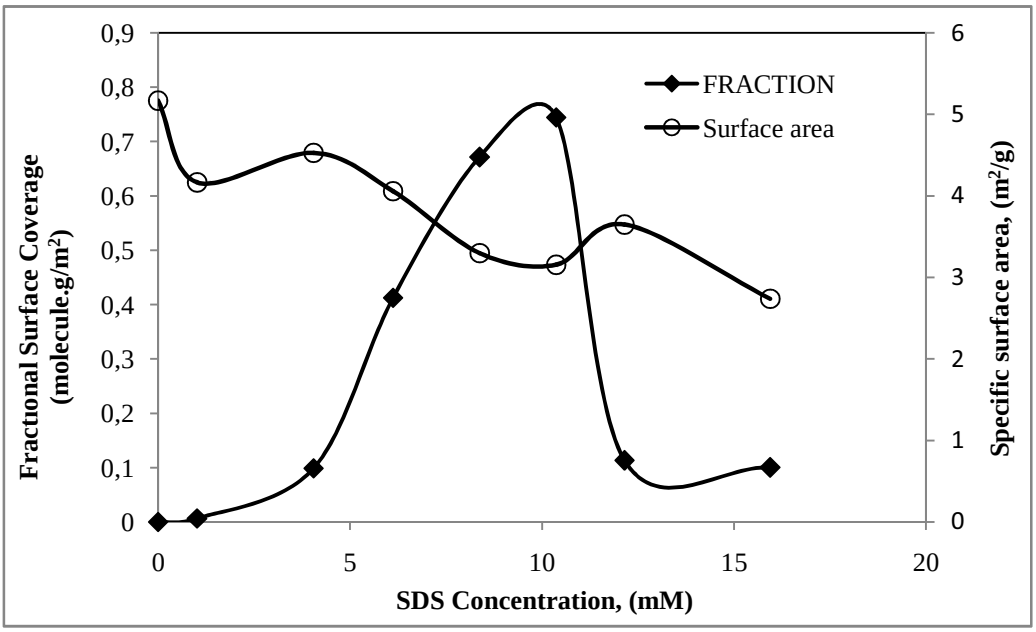

Figure 4.16 Normalized plots of surface area and adsorption.

Fig. 4.15 is replotted in Fig. 4.16 in terms of normalized values where normalized adsorption is defined as the ratio of the amount of SDS adsorbed at any concentration to the SDS adsorbed at CMC, and the normalized surface area as the Surface area of ZnO after adsorption of SDS to the Surface area of ZnO without SDS adsorption.

4.2.2 Adsorption after conditioning of ZnO surfaces

In this case ZnO particles were kept in a solution of given pH, for surface species to form before adsorption.

4.2.2.1 <u>Determination of SDS adsorbed amount at different pH</u>

The amount of SDS adsorbed at different pH is given in Fig. 4. 17, and the section below an SDS concentration of $4x10^{-3}$ M is enlarged in Fig. 4.18.

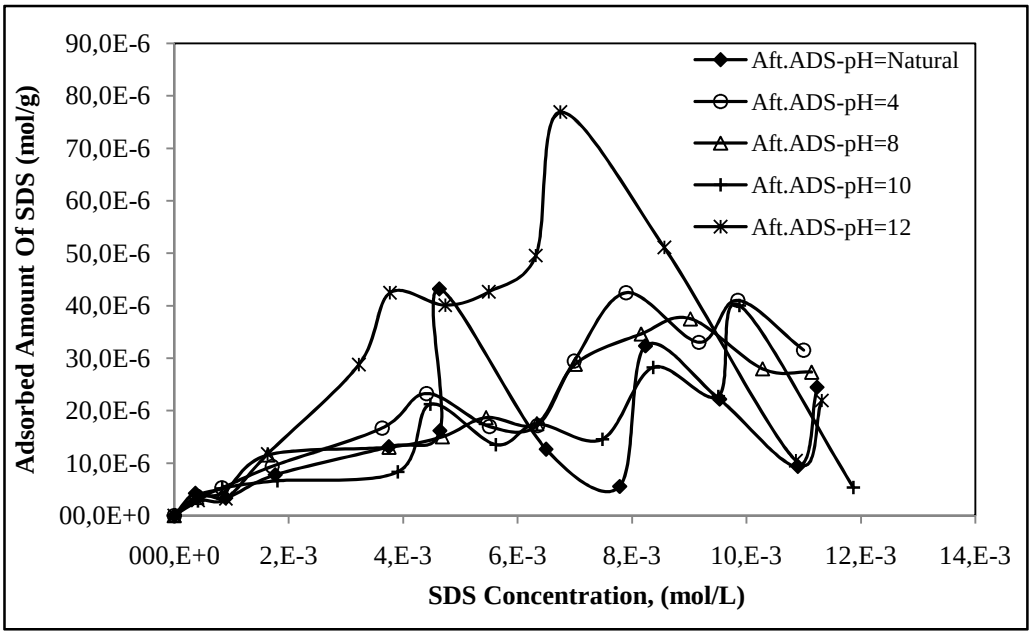

Figure 4.17 The adsorbed amount of SDS at different pH.

As can be observed in Fig. 4.18, the adsorbed amount of SDS is found to decrease with an increase in pH, except for pH 12. Above this concentration SDS adsorption showed flucluations. These results could be obtained only lack of with device sensitivity or surface hydroxyl goups on ZnO which were formed by acid or base solution.

Furthermore, formation of the surface species on ZnO can be other effect of pH to SDS adsorption condition. At high pH value, surface of ZnO was covered with $Zn(OH)_{3\,(aq)}^{-}$ and $Zn(OH)_{4\,(aq)}^{2-}$ according to Eq. 2.10 – 2.11. So, surface of ZnO is negatively charged. According to our experimental results, the isoelectric point of ZnO used in this study is between 8.7 and 11. At high pH, ZnO is negatively charged, anionic sodium dodecyl sulfate can not be adsorbed due to its anionic nature and adsorption of negatively charged SDS on the similarly charged ZnO is very low. Between $6x10^{-3}$ M and $8x10^{-3}$ M SDS adsorbed amount was increased with increase of SDS concentration, maybe it can be interactions between hydrophobic chains of the surfactants take place leading to a rapid rise in adsorption ($4x10^{-3}$ M< conc. < $8x10^{-3}$ M). Above the cmc, the adsorption rate decreased with SDS concentration.

In addition, the dodecanol can be affected the adsorption conditions, because SDS adsorbed amount was decreased with formation of micelles because of the dodecanol was joined in micelle structure. Indeed, joining of the dodecanol

in micelle was accelerated by decreasing of CMC value. So, surface charge regulation was decreased to effect of dodecanol to adsorption. The dodecanol was decreased to SDS adsorption amount after cmc point without charge regulation, but here, adsorbed amount was increased with increasing of SDS concentration.

If values of SDS adsorbed amounts are taken up to $4x10^{-3}$ M, these values will be showed as Fig. 4.18.

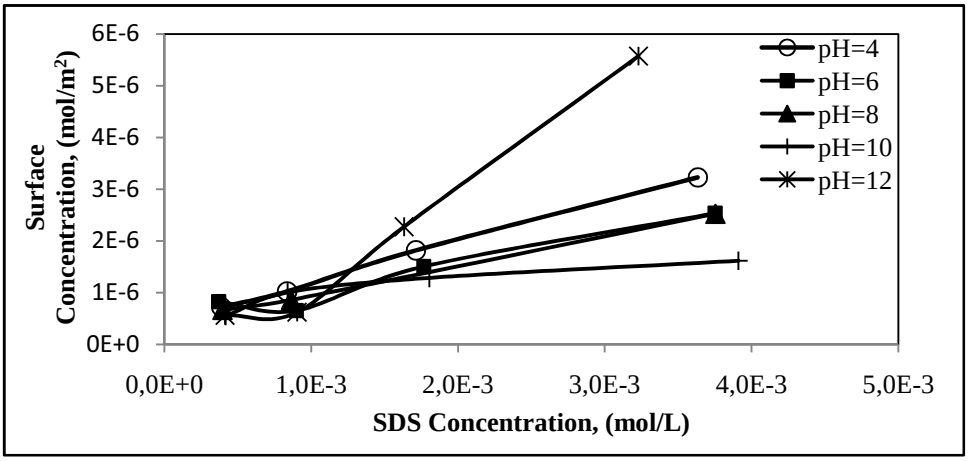

Figure 4.18 Surface concentration of ZnO after adsorption.

In addition, adsorbed amount of SDS was increased with increased of SDS concentration at different pH. As seen Fig.4.19, two adsorption shape have same behaviour.

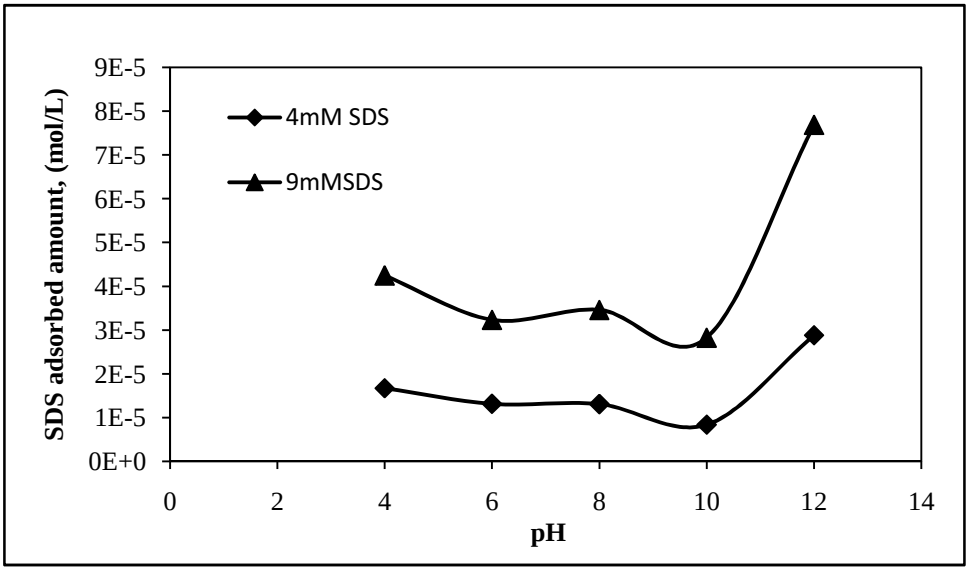

Figure 4.19 Variation of SDS adsorbed amount with pH.

As seen Fig. 4.18, adsorption amount of SDS was decreased with increasing of pH, except pH 12. This assumed Fig. 4.18 coincide with both surface concentration (Fig. 4.20) and surface charge density result (Fig. 4.21).

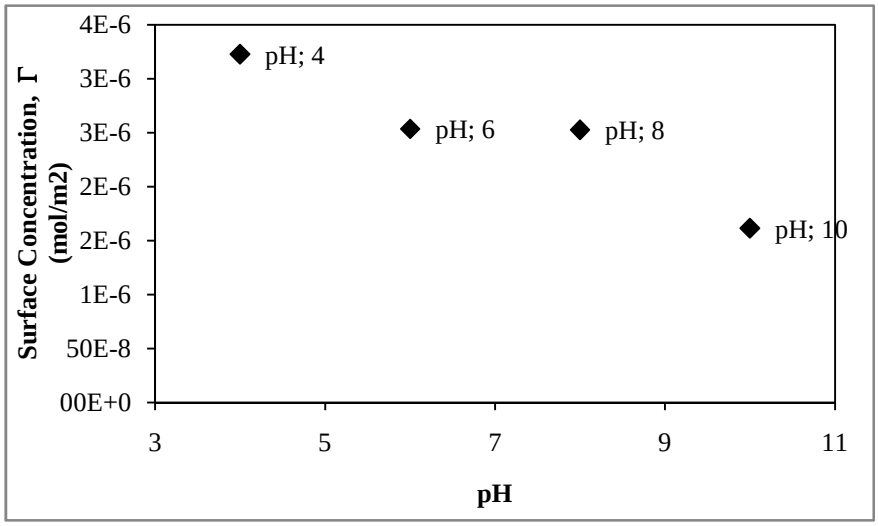

Figure 4.20 Variation of surface concentration of ZnO with pH ($4x10^{-3}$M) .

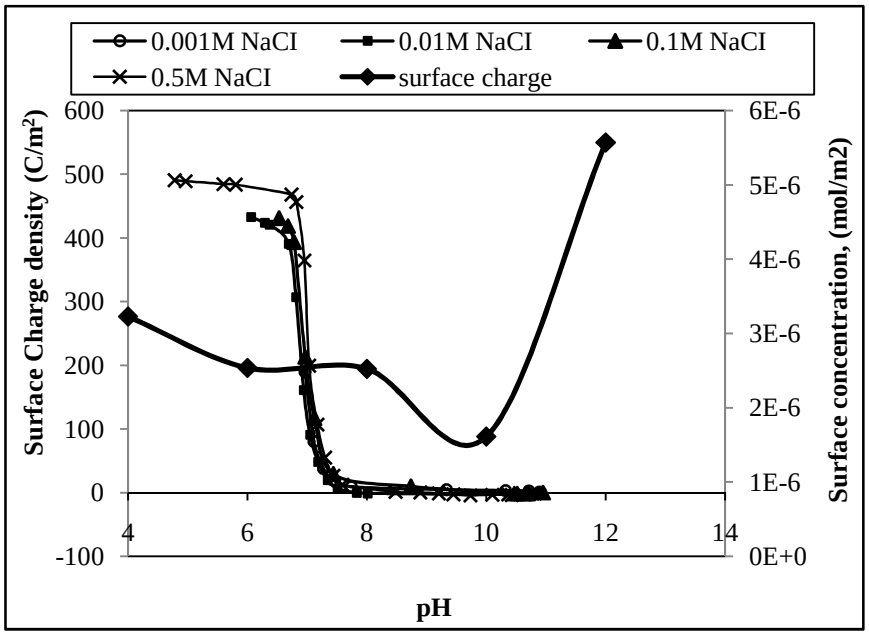

Figure 4.21 The relation between surface charge density of ZnO and surface concentration

Consequently, SDS adsorption onto ZnO can be affected with pH because of forming of surface species on ZnO at different pH.

4.2.3 Determination of pH and Conductivity

In here, experiments made can be shown at two parts as before adsorption and after adsorption. The ‘‘before adsorption’’ term can be explained as conditions of SDS aqueous solutions before adsorption of SDS onto ZnO. The ‘‘after adsorption’’ term can be explained as conditions of SDS aqueous solutions after adsorption of SDS onto ZnO, that is, their supernatant solutions.

4.2.3.1 Before adsorption

Variation of pH of SDS solutions

Firstly, SDS solutions at different concentrations had nearly same pH value in water.

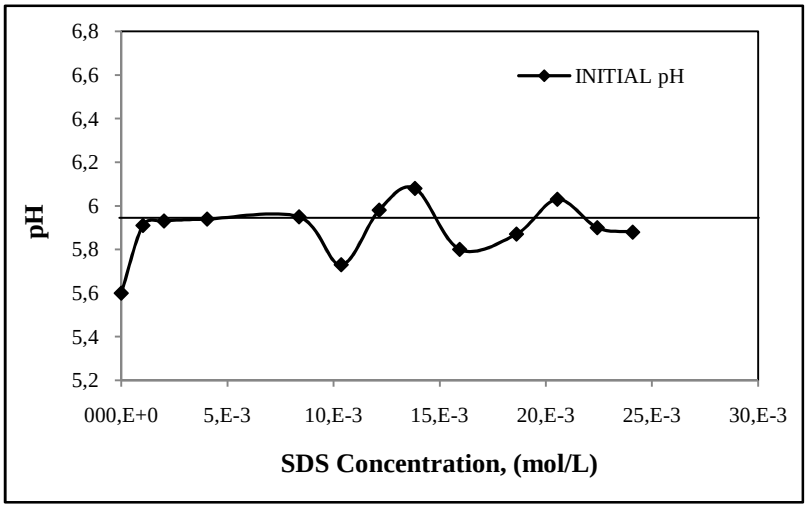

Figure 4.22 pH of SDS solutions at different concentrations.

As seen Fig. 4.22, initial pH value of water was equal to 5.6, than it was increased with added SDS in solution which was nearly fixed to pH 5.9. Indeed, at environment OH^- ions concentration was increased slightly. These results can be occurred from decomposition of SDS in water as Eg. 4.1 (Wang et al., 2005).

$$RSO_4Na + H_20 \rightarrow ROH + SO_4^{2-} + Na^+ + H^+ \quad (4.1)$$

In aqueous solution, as seen Eq. 4.1, H^+ ions can be associated with R group, so solutions pH were increased slightly.

After SDS solutions pH was set to different pH values, new pH values of SDS solution before adsorption were nearly constant as given in Fig. 4.23.

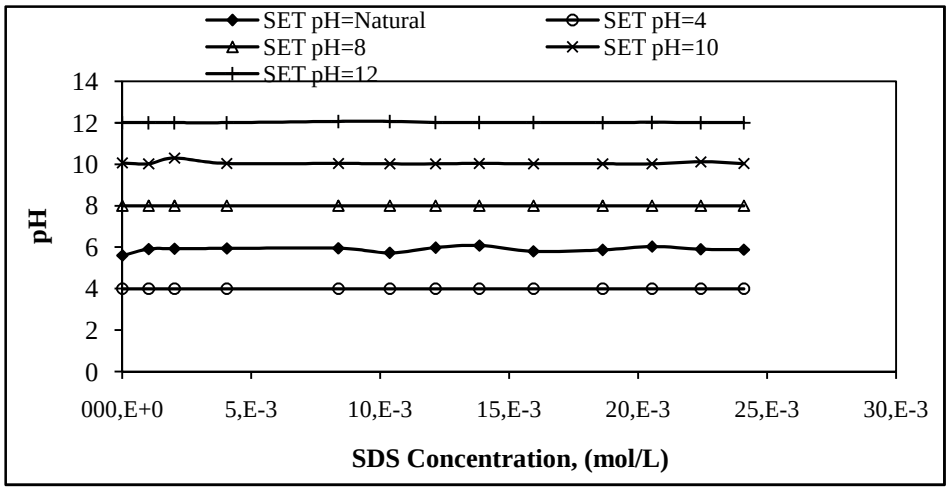

Figure 4.23 pH of SDS solutions after set.

Variation of the conductivity of SDS solutions

According to Fig. 4.24, the CMC value was determined by the intersection of two linear segments on a plot of conductivity versus surfactant concentration. The CMC value of SDS solutions at natural pH, aproximately pH 6 were obtained as $8.3x10^{-3}$M at 25^{o}C compare with literature (Stokes and Evans, 1996; Huang and Lee, 2000). Before absence of any SDS molecules in water, conductivity of water was equal to 1.6 μS/cm. The conductivity of water was increased with added SDS molecules in water, that is, ion effect can be seen from Fig. 4.24 clearly.

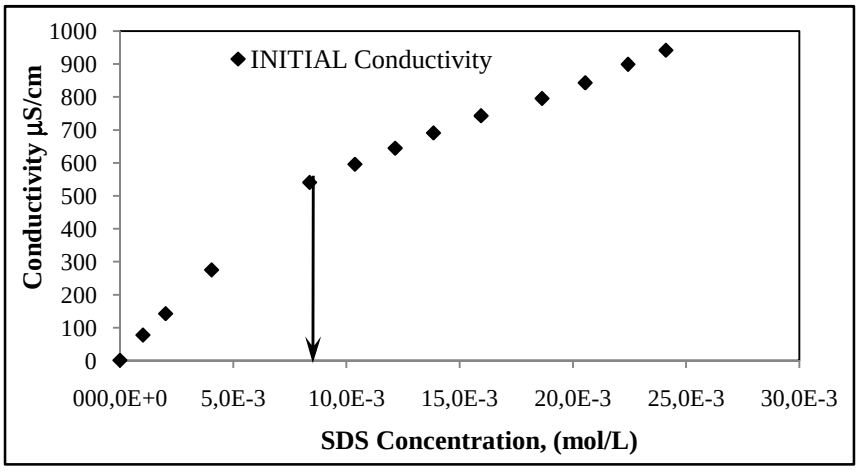

Figure 4.24 Conductivity measurement of SDS solutions.

After the pH of SDS solutions was set to predetermined pH values, new conductivity values of SDS solution before adsorption were obtained as given in Fig. 4.25.

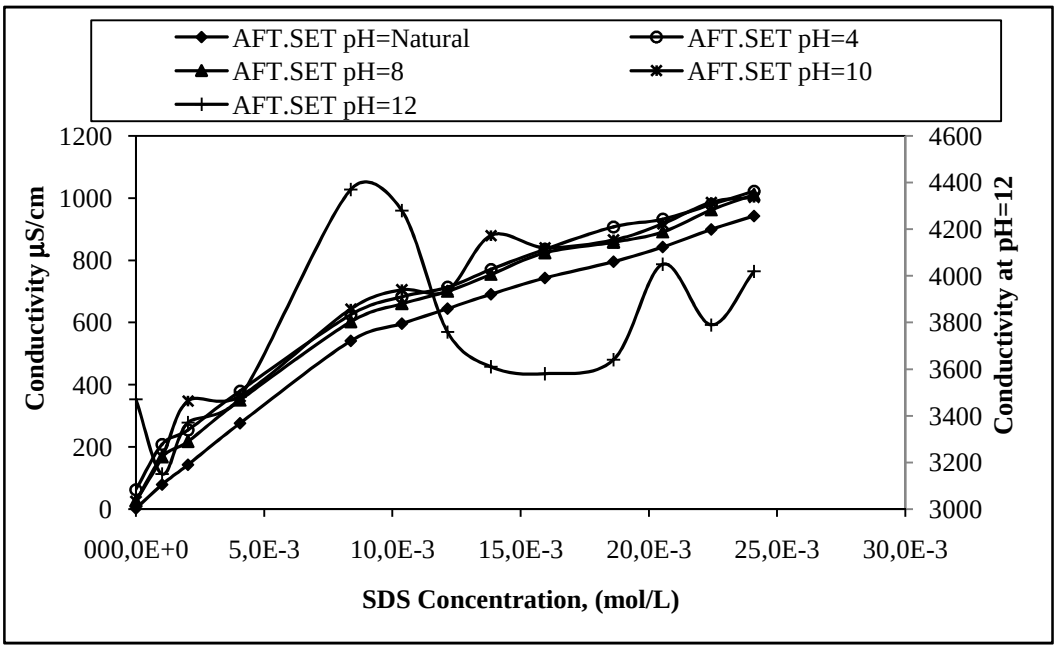

Figure 4.25 Conductivities of SDS solutions after pH set.

As given in Fig. 4.25, conductivities of SDS solutions were affected from adjustment of pH, so the conductivity were changed by OH^- ions easily. It was maximum at pH 12 because of maximum OH^- ions concentration.

Before SDS was added to water, several aqueous solutions at different pH was prepared initially. These solution pH and conductivity values were given in Table 4.3.

Table 4.3 Conductivities of water at different pH values.

Water, pH	Conductivity µS/cm
4	62.5
Natural, 6	1.6
8	14.4
10	25.3
12	3460

As seen Table 4.3, conductivities values of water at different pH were arranged between pH natural as bottom limit and pH 12 as upper limit. After SDS solutions pH set to different values, this ordering didn't change as seen Fig. 4.25.

4.2.3.2 After adsorption

Variation of the pH of SDS solutions

After adsorption of SDS onto ZnO surface, pH of the supernatant solutions were measured as given in Fig. 4.26.

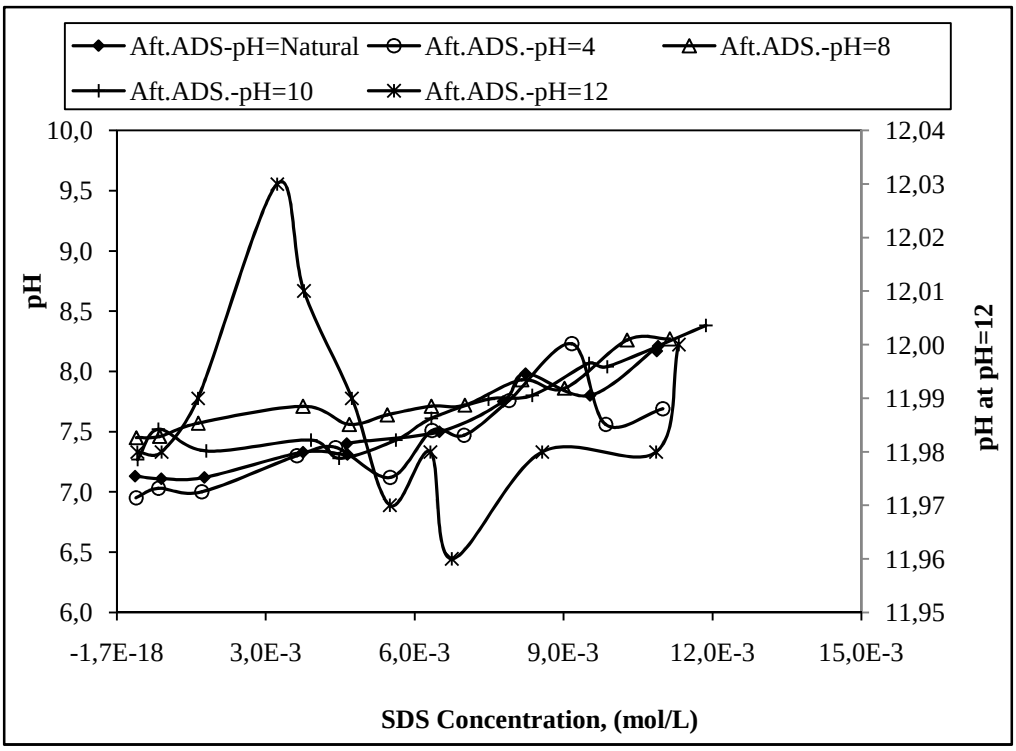

Figure 4.26 pH of supernatant solutions after adsorption.

As can be observed in Figure 4.26, after the adsorption of SDS, pH values of the supernatant solutions were constant between pH 6.9 and pH 8.3 and these pH values increased linearly with an increase in the SDS concentration as lineer, except in the case of pH 12.

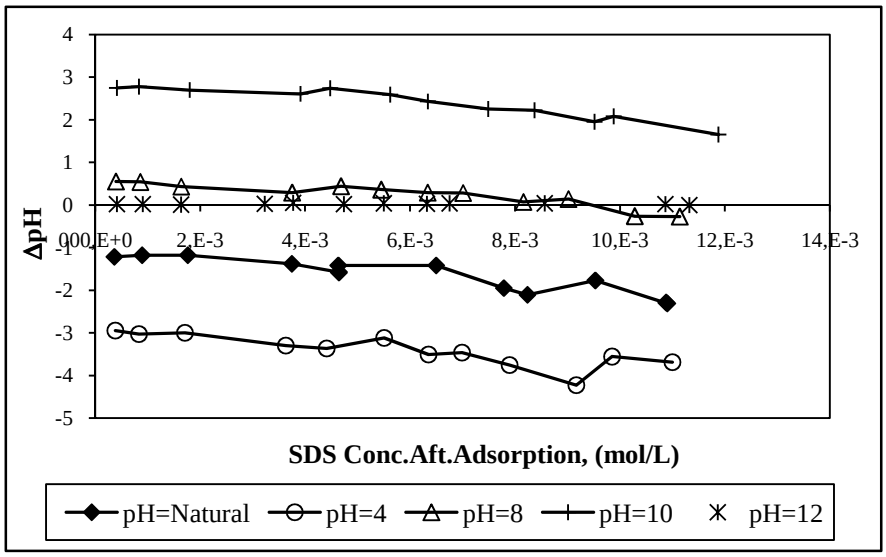

Figure 4.27 Variation of pH with concentration of SDS solutions.

The minimum variation of pH has occurred at pH = 12. These results can be interpreted better if they are plotted as the variation of pH with the SDS concentration in supernatant solution as given in Fig. 4.27. The variation of pH (ΔpH) was obtained as difference in pH of the solution after adsorption and the pH of the solution after being set to constant value, that is, it is the difference between initial and final value. Thus, ΔpH value of SDS solutions at pH 4 and pH natural (6) were negative with increasing SDS concentration (Fig.4.27). Although ΔpH value of pH 4 and pH 6 were increased with an incease in SDS concentration, it was decreased with increasing of SDS concentration at pH = 8 and pH = 10.

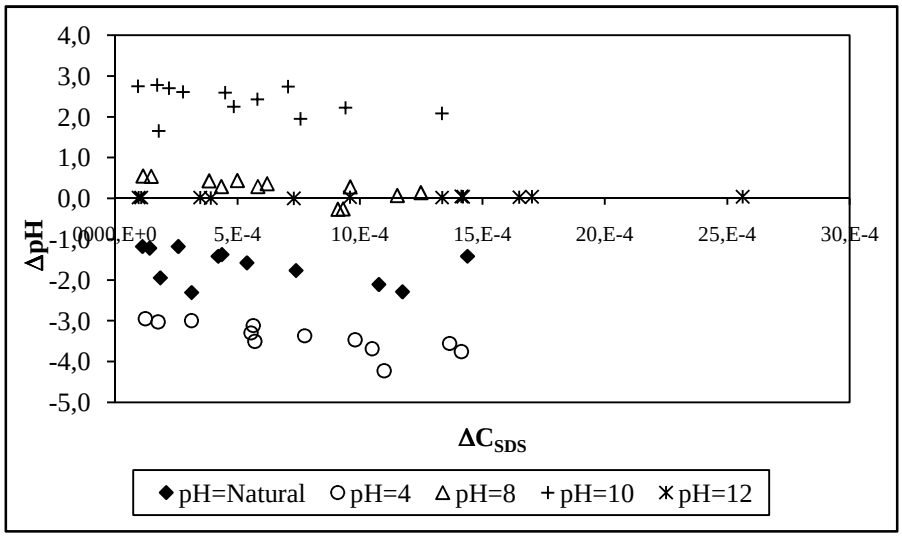

Figure 4.28 Variation of pH with variation of SDS concentration.

Similar results can be observed Fig. 4.28, also. Here, the relation between variation of the pH and SDS concentrations of the solutions can be observed more clearly. The variation of SDS concentration, ΔC_{SDS} is the difference between concentration of SDS solution before and after adsorption. For pH = 4 and pH natural (pH = 6), ΔpH has increased with an increase in ΔC_{SDS} , unlike pH = 8 and pH = 10.

Variation of the conductivity of SDS solutions

In this set of experiments, conductivities of supernatant solutions were obtained after adsorption of SDS onto ZnO surface as given in Fig. 4.29.

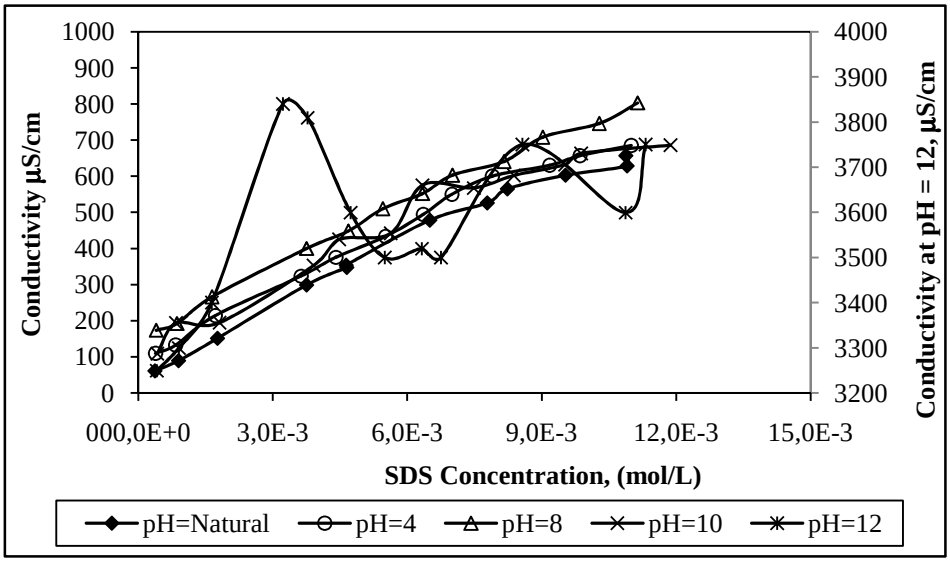

Figure 4.29 Conductivities of SDS solutions after adsorption.

The conductivity values were arranged between pH 6 (natural) and pH 12. In addition to this results same to Fig. 4.24. The values were again minimum at pH 6 and pH 12. As seen Fig. 4.29, Δconductivity was increased linearly until $4x10^{-3}$M SDS concentration, then it can be fixed between for pH 6 – 8, 200 and for pH 4 – 10, 300. The maximum variation of Δconductivity was occured at both pH 4 and pH 10 unlike pH 6 and pH 8.

Because pH and conductivity of SDS solutions were fixed between pH 7 and pH 8 and between conductivity 0 and 1000, respectively after adsorption, the maximum variation values of conductivities were seen pH 4 and pH 10.

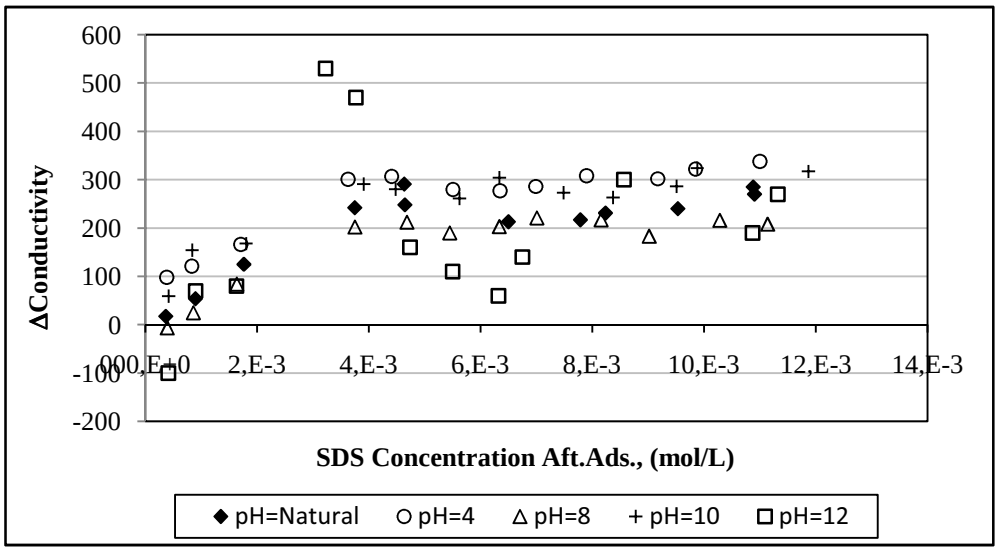

Figure 4.30 Variation of conductivity with concentration of SDS solution after adsorption.

As can be observed in Fig. 4.30, the values of Δconductivities for pH 12 were minimum in particular after $4x10^{-3}$M SDS concentration.

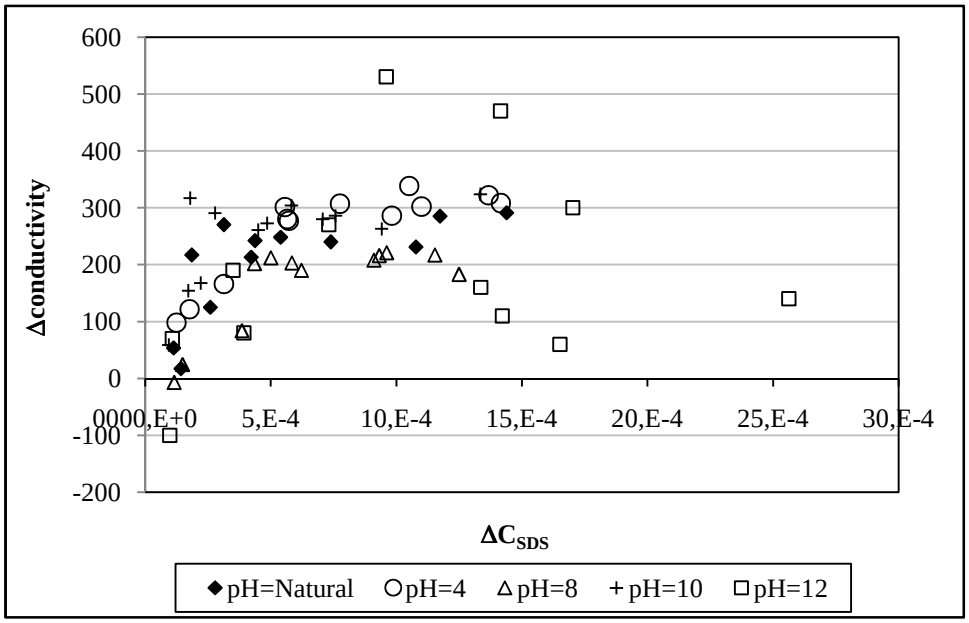

Figure 4.31 Variation of conductivity with variation of concentration of SDS solution after adsorption.

The same results can be seen from Fig. 4.31. Here, the values of Δconductivities were increased with increasing of ΔC_{SDS}. The values of Δconductivities for pH 12 were again minimum.

Consequently, after adsorption of SDS onto ZnO at pH 4 and pH 6, pH of supernatant SDS solution was increased to level of pH 7 - 8. As opposed to pH 4 and pH 6, pH of supernatant SDS solution was decreased to level of pH 7.2 - 8.4 for pH 8 and pH 10. These results can be attributed to the formation of surface species on ZnO in aqueous solution. The surface charge ZnO was found as not stable $8< pH< 12$. In this range, $Zn(OH)_{2(aq)}$ particles are present in the solution.

In addition, pH of the supernatant solution could be affected with the adsorption of SDS onto ZnO. It is possible that, ion exchange has occured between SDS molecules and ZnO hydroxyl groups.

Since the surface charge of ZnO is nearly zero around pH=12, there was no change in the pH of the supernatant solution during the adsorption process. The specific adsorption (mol/g) at pH=12 is much larger than that at other pH values. This excess in adsorption was attributed to a change in the adsorption mechanism. As can be observed in the pH and conductivity figures, variation of pH and conductivity were very stable at pH 12 after adsorption. It is probable that SDS molecules were adsorbed at a neutral surface; that of ZnO surface near the point of zero charge. In this case, the adsorption would be physical through van der Waals forces instead of through charge neutralization.

4.3 Desorption

The desorbed amount of SDS from ZnO surfaces is given in Fig. 4.32. As can be observed from the figure, the desorbed amount of SDS confirmes with adsorbed amount of SDS. Minimum in both adsorption and desorption is observed at pH = 10, or around the isoelectric point.

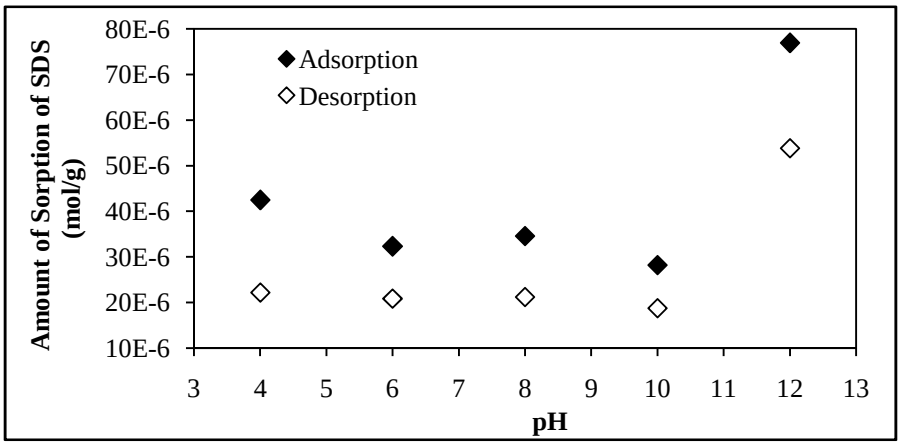

Figure 4.32 Sorption of SDS.

Percent desorption of SDS as $\left(\frac{m_{des.}}{m_{ads.}} x100\right)$ is given in Fig. 4.33 as a function of pH of the solution at which adsorption and almost a linear as observed in the % desorption with pH.

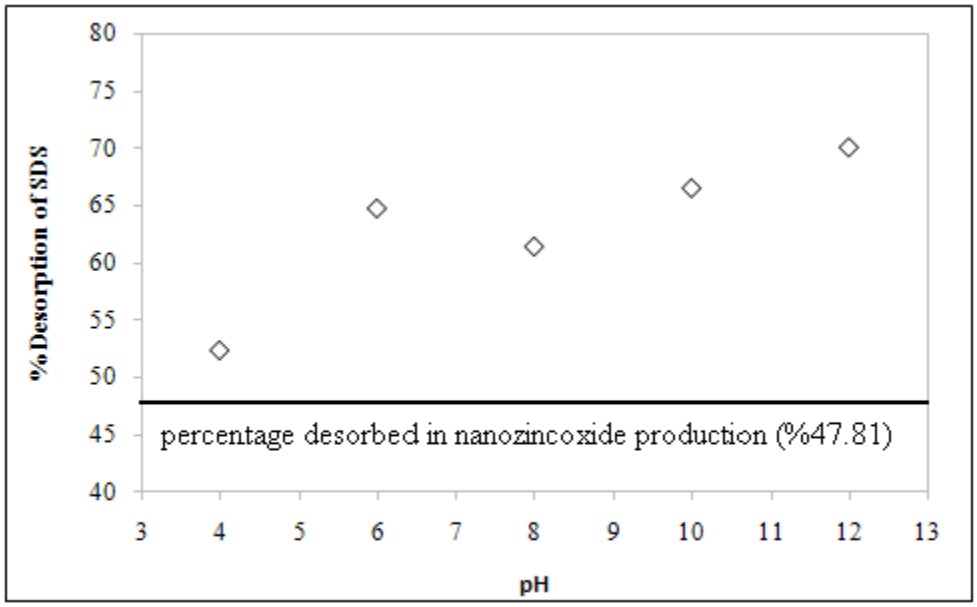

a)

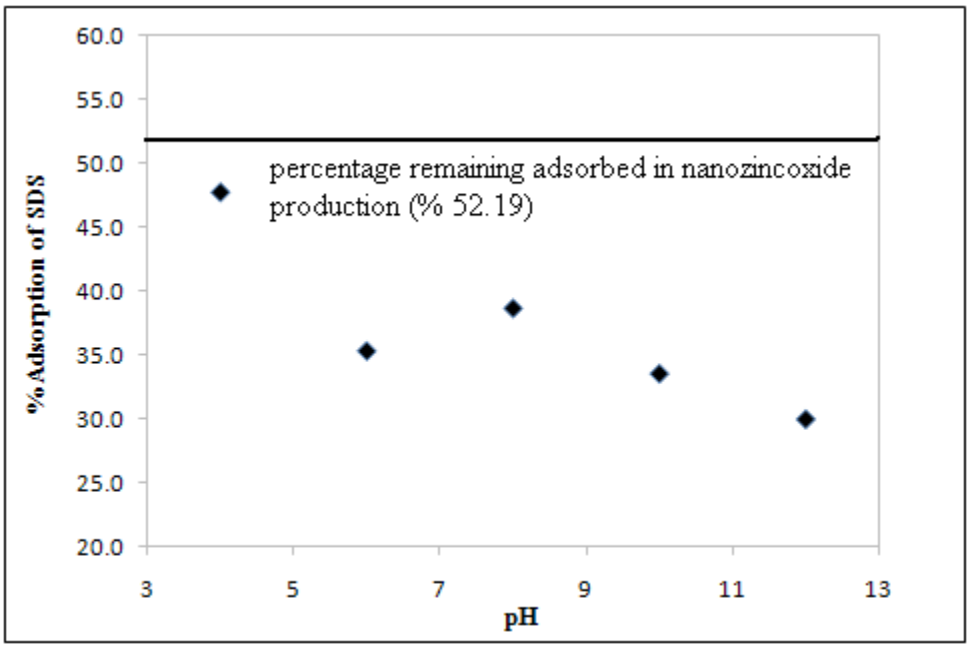

b)

Figure 4.33 a) % SDS desorbed. b) % remaining adsorbed after washing.

The strongest interaction between SDS and ZnO is found at pH = 4 because of charge regulation. The least interaction between SDS and ZnO is found at pH = 12 (Fig. 4.33 a), where the adsorption is mainly through van der Waals forces. The line through 47.81 % gives the percent desorption obtained in washing

the ZnO nanoparticles with water, after the reaction in the autoclave. The difference in the percent desorption found in this work and that in ZnO nanoparticle production probably arises from the SDS chemisorbed into the O-vacancies in the crystal structure during the formation of the nanoparticles. Formation of ZnO took place at around pH = 13 and washing was done with water at the natural pH (pH = 6). Thus, the desorption percentage ranges between 65 and 70 in this interval, corresponding to approximately 50 % more desorption.

5. CONCLUSION

Adsorption of SDS on ZnO surfaces is important from the standpoint of surface purity of ZnO.

Many metal oxides will hydrolize in the presence of water to form hydroxide layers at the surface (≡ M-OH). Water molecules may be both physically and chemically adsorbed onto the surface of the dispersed oxide particles. The polar hydroxyl (-OH) groups may cause the surface to attract and physically adsorb a single or several additional layers of polar water molecules. An oxide or hydroxide surface (≡ M-OH) can become charged by reacting with H^+ or OH^- ions due to surface amphoteric reactions. The adsorption of SDS onto ZnO can be considered as solid – liquid process of adsorption, so the properties of aqueous SDS (as adsorbate) solution condition and the properties of solid ZnO (as adsorbent) surface in aqueous solution are important parameters.

In this study, experimental measurements were carried out in the light of the information. In all the experimentals, distilled water at pH 5.58 and conductivity 1.7 μS/cm that contained no additives was used medium temperature, 25^oC.

When the anionic surfactant, sodium dodecyl sulfate (SDS) was added to water, the pH of the solutions were slightly increased to pH 5.9. This result could be due to the solubilization of SDS in water and formation of dodecanol ($C_{12}H_{25}OH$) in the aqueous solution. Dodecanol interact with H^+ ions, decreasing the H^+ concentration in the medium.

The specific surface area (BET) of ZnO was found as 5.17 m^2/g. The crystal structure of ZnO was found with XRD analysis as a wurtzite crystal and the peak of ZnO was the same as the literature results. The particle shape and size of ZnO was obtained with SEM analysis as a short cylinders with hexagonal cross sections and their dimensions were in the order of nanometers. So, it was decided that commercial ZnO could be used to simulate the ZnO produced in the project.

When the ZnO particles were immersed in water, pH of water increased to pH 7.75 due to formation of surface hydroxyl groups, with a resultant decrease in H^+ ions in solution. In the range $7.75 < pH < 12.3$ the pH changed as a function of time due to formation of unstable colloidal particles of $Zn(OH)_{2(aq)}$. During $Zn(OH)_{2(aq)}$ transformation, consumption of hydroxyl ions from the solution takes

place and lowers the final equilibrium pH of the zinc oxide suspension. The results confirm with literature (Degen, A. and Kosec, M., 2000).

At pH < 5.5, solubility of ZnO was increased with a decrease of pH value, that is, concentration of Zn^{++} ions was increased and was maximum at pH 2. The minimum solubility of ZnO occurrs in the range 9.5 < pH < 12. The concentration of Zn^{++} ions increases again after pH > 12. This result also confirms with literature results (Sedlak, A. and Janusz, W., 2008).

The surface charge density of the zinc oxide particles was examined at different electrolyte concentrations. The surface charge density of ZnO was affected by both pH and electrolyte concentration. The point of zero charge (pzc) values of ZnO was determined as 8.76, 10.7 and 11 for 0.5M, 0.1M and 0.001M electrolyte solution, respectively. This result is in agreement with literature values (Sedlak, A. and Janusz, W., 2008).

Initially SDS adsorption onto ZnO at natural pH (pH = 5.9) were done without surface charge conditioning. In these experiments, the maximum adsorption was found around the CMC. At higher concentrations, adsorption of SDS decreased rapidly. This result could be due to solubilization of dodecanol in micelles. The dodecanol contributed to SDS adsorption on ZnO, so decreasing of dodecanol amount in solution decreased the adsorbed amount of SDS. These results were supported with BET and EDS analysis. The BET analysis was found to be inversely proportional with the adsorbed amount of SDS. In the EDS measurements, concentration of sulphur ions on ZnO were increased with in increase in the adsorbed amount of SDS.

In the second set of experiments of SDS adsorption onto ZnO at different pH value were performed with surface charge conditioning. Here, the adsorbed amount of SDS was found to decrease with an increase in the pH value, except in the case of pH 12. The maximum adsorption was found at pH 4 and the minimum adsorption amount of SDS was determined at pH 10, except in the case of pH 12. The surface charge of ZnO was affected from pH, so at low pH, adsorption was maximum because of positive surface charge of ZnO and at high pH values, adsorption was minimum because of negative surface charge of ZnO. In case of pH 12, adsorption of SDS was increased with an increase in pH. Surface charge reversal could lead to an increase in the adsorbed amount of SDS. This pH value is near the point of zero charge of ZnO, so that the surfaces charge of ZnO can be

electrostatically neuter. Adsorption of SDS onto ZnO would then increase with increasing concentration of SDS due to physical adsorption.

After adsorption, pH and conductivities of SDS solutions reached equilibrium $7 < pH < 8$ and conductivity 1.6 – 1000 μS/cm, respectively. In case of pH 12, variation of pH and conductivity were wery low. However, at pH 4 and 6, pH of supernatant solutions were increased with increasing the amount of SDS adsorbed and at pH 8 and 10, pH of supernatant solutions were decreased with an increase in the amount of SDS adsorbed. These results show that, the H^+ and OH^- ions are exchanged between ZnO surface and aqueous phase.

The desorption of SDS from ZnO surface was conducted by aqueous solutions at the same pH as in the adsorption conditions. The strongest interaction between SDS and ZnO was found to be at pH = 4, observed as a minimum in the desorbed percentage of SDS. The least interaction between SDS and ZnO was found at pH = 12, as evidenced by the maximum in desorbed percentage of SDS. So, interaction between SDS and ZnO declined with an increase in the pH. In this study, desorbed amount of SDS was found to be higher than desorption percentage in the washing step of the nanoparticle production. The difference in the desorbed amounts could be due to the SDS chemically bonded with ZnO surfaces, at the –O– vacancies during the formation of crystals.

APPENDICES

APPENDIX A. SOLUBILITY OF ZnO

Table A.1 Determination of solubility of ZnO by variation of pH.

pH	Solubility Perc.of Zn^{++} (mol/mol ZnO) (%)	
	First	**Repetition**
2.0	1.197	1.1973
3.0	0.075	0.0752
3.5	0.022	0.0218
4.0	0.010	0.0100
4.5	0.009	0.0090
5.0	0.007	0.0066
5.67	0.005	0.0046
6.0	0.008	0.0080
6.5	0.005	0.0046
7.0	0.005	0.0047
7.5	0.005	0.0055
8.0	0.006	0.0063
8.5	0.005	0.0047
9.0	0.005	0.0052
9.5	0.003	0.0034
10.0	0.003	0.0031
11.0	0.001	0.0018
12.0	0.001	0.0003
13.0	0.075	0.0751

APPENDIX B. STABILITY OF pH

Table B.1 Determination of the stable region by variation of pH.

PH_{PRESET}	PH_{FINAL}					
4	4	**1.day**	**2.day**	**3.day**	**4.day**	**Concentration of Zn^{++} (mg/L)**
5	5					
5.12	5.12	5.23	5.23	5.26	5.26	48500
6	6	5.96	6.06	6.06	6.04	7500
6.99	6.99	6.91	6.89	6.88	6.89	1000
8.01	8.01	7.99	7.98	7.91	7.87	13.3
9	9	8.51	8.5	8.47	8.46	5.5
10	10	9.67	9.34	9.19	9.1	1.5
11.01	11.01	10.43	10.34	10.23	10.14	2.3
12.03	12.03	11.98	11.99	11.98	11.96	2
12.5	12.5					
12.8	12.8					

APPENDIX C. SURFACE CHARGE DENSITY OF ZnO

Table C.1 Determination of surface charge density of ZnO, for 0.001 M NaCI.

ZnO		0.001M NaCI			
pH	**V (mL)**	**pH**	**V (mL)**	**ΔV**	**Surface Charge density (C/m^2)**
10.91	1.8	10.91	1.4	0.4	0.7
10.88	2.4	10.88	2.0	0.4	0.8
10.71	5.5	10.71	4.4	1.1	2.1
10.32	10.2	10.32	8.3	1.9	3.5
9.33	14.5	9.33	11.9	2.6	4.9
7.74	17.9	7.74	12.8	5.0	9.4
7.43	24.0	7.43	13.2	10.9	20.3
7.27	33.8	7.27	13.3	20.4	38.1
7.11	56.7	7.11	13.5	43.2	80.6
6.96	115.5	6.96	13.7	101.7	189.9

Table C.2 Determination of surface charge density of ZnO, for 0.01 M NaCI.

ZnO		0.01M NaCI			
pH	**V (mL)**	**pH**	**V (mL)**	**ΔV**	**Surface Charge density (C/m^2)**
10.85	1.5	10.85	2.2	-0.7	-1.2
10.81	2.1	10.81	2.8	-0.7	-1.3
10.6	4.4	10.6	5.8	-1.4	-2.6
8.01	14.5	8.01	15.2	-0.7	-1.4
7.83	15.2	7.83	15.4	-0.1	-0.2
7.51	19.0	7.51	15.7	3.3	6.2
7.34	26.5	7.34	15.9	10.6	19.8
7.18	42.1	7.18	16.1	26.0	48.6
7.05	65.2	7.05	16.3	48.9	91.2
6.94	102.9	6.94	16.5	86.4	161.2
6.81	181.4	6.81	16.8	164.6	307.1
6.69	226.4	6.69	17.1	209.3	390.6
6.37	243.6	6.37	18.2	225.4	420.8
6.29	245.5	6.29	18.5	227.0	423.7
6.06	251.4	6.06	19.4	232.0	433.1

Table C.3 Determination of surface charge density of ZnO, for 0.1 M NaCI.

ZnO		0.1M NaCI			
pH	**V (mL)**	**pH**	**V (mL)**	**ΔV**	**Surface Charge density (C/m^2)**
10.95	0.9	10.95	1.0	-0.04	-0.08
10.7	4.6	10.7	5.4	-0.80	-1.50
10.66	5.2	10.66	6.0	-0.82	-1.52
10.52	6.9	10.52	7.7	-0.83	-1.55
10.47	7.5	10.47	8.3	-0.83	-1.55
8.74	20.4	8.74	15.3	5.17	9.66
7.44	31.6	7.44	16.0	15.69	29.29
7.12	79.0	7.12	16.3	62.75	117.13
6.97	130.5	6.97	16.4	114.08	212.94
6.78	227.4	6.78	16.6	210.74	393.35
6.68	241.0	6.68	16.8	224.24	418.55
6.53	247.9	6.53	17.0	230.82	430.83

Table C.4 Determination of surface charge density of ZnO, for 0.5 M NaCI.

ZnO		0.5M NaCI			
pH	**V (mL)**	**pH**	**V (mL)**	**ΔV**	**Surface Charge density (C/m^2)**
10.81	3.6	10.81	4.2	-0.60	-1.11
10.77	4.2	10.77	4.8	-0.63	-1.17
10.63	5.9	10.63	7.3	-1.35	-2.51
10.42	8.2	10.42	10.3	-2.07	-3.86
10.37	9.3	10.37	10.9	-1.55	-2.89
10.01	12.0	10.1	13.7	-1.66	-3.11
9.73	14.8	9.73	16.9	-2.15	-4.01
9.45	17.5	9.45	19.0	-1.43	-2.67
9.2	19.7	9.2	20.4	-0.71	-1.32
8.89	21.7	8.89	21.7	0.03	0.05
8.48	23.4	8.48	22.6	0.76	1.42
7.59	30.2	7.59	23.6	6.62	12.35
7.44	37.8	7.44	23.8	13.98	26.10
7.3	53.432	7.3	24.006	29.43	54.92
7.17	81.682	7.17	24.24	57.44	107.22
7.03	131.186	7.03	24.496	106.69	199.14
6.95	220.26	6.95	24.758	195.50	364.91
6.82	269.782	6.82	25.126	244.66	456.66
6.74	276.136	6.74	25.464	250.67	467.89
5.8	290.178	5.8	31.15	259.03	483.49

Table C.5 Determination of the surface concentration of ZnO after adsorption by variation of pH.

pH	Surface Concentration (mol/m^2)
4	3.23E-06
6	2.54E-06
8	2.52E-06
10	1.61E-06
12	5.57E-06

APPENDIX D. BET ANALYSIS

Table D.1 Determination of BET area of ZnO variation of SDS adsorbed amount.

SDS Conc. (mM)	Surface Area (m^2/g)	Adsorbed mol of SDS (mol/gZnO)	Surface Concentration, (mol/m^2)
0.00	5.17	0	0
1.02	4.17	3.39E-07	8.14125E-08
4.05	4.53	5.92E-06	1.30634E-06
6.12	4.06	1.98E-05	4.88194E-06
8.37	3.30	2.13E-05	6.4567E-06
10.37	3.16	2.16E-05	6.84935E-06
12.14	3.65	4.40E-06	1.20506E-06
15.94	2.74	2.19E-06	8.00116E-07

Table D.2 Determination of surface coverage of ZnO by SDS.

SDS Conc. (mM)	Fractional Surface Coverage ($1/m^2$)
0.00	0.00
1.02	0.01
4.05	0.10
6.12	0.41
8.37	0.67
10.37	0.74
12.15	0.11
15.94	0.10

Table D.3 Amount of Zn^{++} ions in supernatant solutions.

SDS Conc. (mM)	**Concentration of Zn^{++}(mg/L)**
0.00	1.85
1.02	16.6
4.05	22.00
6.12	19.40
8.37	27.20
10.37	21.60
12.14	36.40
15.94	52.00

APPENDIX E. ADSORPTION OF SDS AT NATURAL pH

Table E.1 Adsorbed amount of SDS onto ZnO at constant pH.

Sample Conc.(M)	Adsorbed mol of SDS onto ZnO (mol/g)
1.06E-03	1.65E-06
2.06E-03	2.61E-06
3.99E-03	4.08E-06
5.99E-03	1.58E-05
8.21E-03	1.64E-05
1.02E-02	1.60E-05
1.24E-02	5.31E-06
1.62E-02	2.67E-06

APPENDIX F. ADSORPTION OF SDS AT DIFFERENT pH

Table F.1 Adsorption at pH 4.

pH=4			
AFTER ADSORPTION			
Sample Conc.(M)	**pH**	**Conductivity µS/cm**	**Adsorbed Amount of SDS (mol/g)**
3.86E-04	6.95	110	03.74E-6
8.34E-04	7.03	132	05.29E-6
1.71E-03	7.00	214	09.39E-6
3.63E-03	7.30	324	16.68E-6
4.41E-03	7.37	376	23.26E-6
5.51E-03	7.12	433	16.96E-6
6.35E-03	7.51	494	17.16E-6
6.99E-03	7.47	550	29.45E-6
7.90E-03	7.76	600	42.47E-6
9.17E-03	8.23	630	33.00E-6
9.85E-03	7.56	657	41.01E-6
1.10E-02	7.69	685	31.53E-6

pH=4		
	After set , pH=4	
ΔC_{SDS}	**Conductivity µS/cm**	**ΔpH**
1.2E-4	208	-2.95
1.8E-4	254	-3.03
3.1E-4	380	-3.0
5.6E-4	625	-3.3
7.8E-4	683	-3.37
5.7E-4	713	-3.12
5.7E-4	771	-3.51
9.8E-4	836	-3.47
1.4E-3	908	-3.76
1.1E-3	932	-4.23
1.4E-3	979	-3.56
1.1E-3	1023	-3.69

Table F.2 Adsorption at pH 6 (Natural).

pH=Natural			
AFTER ADSORPTION			
Sample Conc.(M)	pH	**Conductivity µS/cm**	ADSORBED AMOUNT OF SDS (mol/g)
3.68E-04	7.13	61.1	04.26E-6
8.98E-04	7.11	89.4	03.37E-6
1.77E-03	7.12	151.3	07.77E-6
3.75E-03	7.33	299	13.11E-6
4.65E-03	7.31	348	16.18E-6
4.63E-03	7.4	354	43.18E-6
6.50E-03	7.5	478	12.66E-6
7.79E-03	7.75	526	05.57E-6
8.24E-03	7.98	565	32.33E-6
9.53E-03	7.8	603	22.17E-6
1.09E-02	8.21	629	09.39E-6
1.09E-02	8.17	657	35.22E-6

pH=Natural			
	Initial pH		
ΔC_{SDS}	pH	**Conductivity µS/cm**	ΔpH
1.4E-04	5.9	78.2	-1.2
1.1E-04	5.9	142.8	-1.2
2.6E-04	5.9	276	-1.2
4.4E-04	6.0	541	-1.4
5.4E-04	5.7	596	-1.6
1.4E-03	6.0	645	-1.4
4.2E-04	6.1	691	-1.4
1.9E-04	5.8	743	-2.0
1.1E-03	5.9	796	-2.1
7.4E-04	6.0	843	-1.8
3.1E-04	5.9	899	-2.3
1.2E-03	5.9	942	-2.3

Table F.3 Adsorption at pH 8.

pH=8			
AFTER ADSORPTION			
Sample Conc.(M)	**pH**	**Conductivity µS/cm**	**ADSORBED AMOUNT OF SDS (mol/g)**
3.95E-04	7.45	173.8	03.45E-6
8.62E-04	7.46	192.4	04.45E-6
1.64E-03	7.57	266	11.55E-6
3.75E-03	7.71	400	13.05E-6
4.69E-03	7.56	448	15.01E-6
5.45E-03	7.64	510	18.67E-6
6.34E-03	7.71	552	17.52E-6
7.01E-03	7.72	603	28.85E-6
8.16E-03	7.93	641	34.61E-6
9.02E-03	7.86	708	37.50E-6
1.03E-02	8.26	746	27.96E-6
1.11E-02	8.27	803	27.33E-6

pH=8		
	After set, pH=8	
ΔC_{SDS}	**Conductivity µS/cm**	**ΔpH**
115.E-6	167.2	0.55
148.E-6	217	0.54
385.E-6	350	0.43
435.E-6	602	0.29
500.E-6	660	0.44
622.E-6	700	0.36
584.E-6	755	0.29
962.E-6	824	0.28
1.E-3	858	0.07
1.E-3	891	0.14
932.E-6	962	-0.26
911.E-6	1011	-0.27

Table F.4 Adsorption at pH 10.

pH=10			
AFTER ADSORPTION			
Sample Conc.(M)	**pH**	**Conductivity µS/cm**	**ADSORBED AMOUNT OF SDS (mol/g)**
4.16E-04	7.27	109	02.82E-6
8.38E-04	7.52	193.8	05.17E-6
1.80E-03	7.34	194.4	06.63E-6
3.91E-03	7.43	353	08.34E-6
4.48E-03	7.28	425	21.22E-6
5.62E-03	7.43	442	13.51E-6
6.34E-03	7.61	576	17.46E-6
7.49E-03	7.77	568	14.57E-6
8.37E-03	7.8	602	28.25E-6
9.51E-03	8.07	632	22.74E-6
9.88E-03	8.04	663	40.05E-6
1.19E-02	8.38	686	05.37E-6

pH=10			
	After set , pH=10		
ΔC_{SDS}	**pH**	**Conductivity µS/cm**	**ΔpH**
94.E-6	10.02	167.7	2.75
172.E-6	10.3	348	2.78
221.E-6	10.04	362	2.7
278.E-6	10.04	644	2.61
707.E-6	10.02	705	2.74
450.E-6	10.02	703	2.59
582.E-6	10.04	880	2.43
486.E-6	10.02	841	2.25
942.E-6	10.02	865	2.22
758.E-6	10.02	918	1.95
1.E-3	10.12	987	2.08
179.E-6	10.03	1003	1.65

Table F.5 Adsorption at pH 12.

pH=12			
AFTER ADSORPTION			
Sample Conc.(M)	**pH**	**Conductivity µS/cm**	**ADSORBED AMOUNT OF SDS (mol/g)**
4.13E-04	11.98	3250	02.91E-6
9.03E-04	11.98	3300	03.22E-6
1.63E-03	11.99	3400	11.76E-6
3.23E-03	12.03	3840	28.80E-6
3.77E-03	12.01	3810	42.46E-6
4.74E-03	11.99	3600	40.09E-6
5.50E-03	11.97	3500	42.66E-6
6.32E-03	11.98	3520	49.55E-6
6.75E-03	11.96	3500	76.91E-6
8.57E-03	11.98	3750	51.09E-6
1.09E-02	11.98	3600	10.47E-6
1.13E-02	12	3750	21.93E-6

pH=12			
	After set , pH=12		
ΔC_{SDS}	**pH**	**Conductivity µS/cm**	**ΔpH**
97.2E-6	12	3150	0.02
1.1E-4	12	3370	0.02
3.9E-4	12	3480	0.01
9.6E-4	12.06	4370	0.03
14.2E-4	12.06	4280	0.05
13.4E-4	12.01	3760	0.02
14.2E-4	12.01	3610	0.04
16.5E-4	12.01	3580	0.03
25.6E-4	12	3640	0.04
17.0E-4	12.02	4050	0.04
3.5E-4	12	3790	0.02
7.3E-4	12	4020	0.00

REFERENCES

Chen, M., Burgess, I. and Lipkowski, J., 2009, Potential controlled surface aggregation of surfactants at electrode surfaces – A molecular view, *Surface Science*, 603:1878-1891.

Degen, A. And Kosec, M., 2000, Effect of pH and impurities on the surface charge of zinc oxide in aqueous solution, *Journal of the European Ceramic Society*, 20:667-673.

Diebold, U., Koplitz, L.V. and Dulub, O., 2004, Atomic-scala properties of low-index ZnO surfaces, *Applied Surface Science,* 237:336-342.

Hu, K. and Bard, J.A., 1997, Characterization of Adsorption of Sodium Dodecyl Sulfate on Charge-Regulated Substrates by Atomic Force Microscopy Force measurements, Langmuir, Texas, 7p.

Huang, J.H., Zeng, G.M., Qu, Y.H. and Zhang, Z., 2007, Adsorption characteristics of zinc ions on sodium dodecyl sulfate in process of micellar-enhanced ultrafiltration, *Trans. Nonferrous Met. Soc. China, 17:1112-1117.*

Huang, L.H. and Lee, G.M.W., 2001, enhanced naphalene solubility in the presence of sodium dodecyl sulfate: effect of critical micelle concentration, *Chemosphere*, 44:963-972.

Jönsson, B. and Lindman, B., 1998, Surfactants and Polymers in Aqueous Solution, John Wiley and Sons Ltd, England, 438p.

Kaplan, F., 2009, Adsorption, power point presentation,10p.

Kosmulski, M., 2009, pH-dependent surface charging and points of zero charge. IV. Updateand new approach, Journal of Colloid and Interface Science, 10p.

Levchenko, A.A., Argo, B.P., Vidu, R, Talroze, R.V. and Stroeve, P., 2002, Kinetics of Sodium Dodecyl Sulfate adsorption on and desorption from Self-Assembled Monolayers Measured by Surface Plasmon Resonance, Langmuir, California, 7p.

Nagao, M. and Morimoto, T., 1980, Adsorption of Alcohols on Zinc Oxide Surfaces, J. Phys. Chem., Okayama, 4p.

Noei, H., Qiu, H., Wang, Y., Löffler, E., Wöll, C. and Muhler, M., 2008, The idendification of hydroxyl groups on ZnO nanoparticles by infrared spectroscopy, *Chem. Phys.*,10:7092-7097.

Oscik, J., 1982, Adsorption, (Trans. I.L. Cooper.), School of Chemistry University of Newcastle upon Tyne, England, 206p.

REFERENCES (continued)

Peterson, R.B., Fields, C.L. and Gregg, B.A., 2004, Epitaxial Chemical Depositon of ZnO Nanocolumns from NaOH Solutions, Langmuir, Colorado, 5p.

Purakayastha, D.P., Pal, A. and Bandyopadhyay, M., 2005, Sorption kinetic of anionic surfactant on to waste tire rubber granules, *Separation and Purification Technology*, 46:129-135.

Reichle, A.R, McCurdy, G.K. and Hepler, G.L., 1975, Zinc Hydroxide: Solubility Product and Hydroxy-complex Stability Constants from 12.5-75^{o}C, Can. J. Chem., Lethbridge, 4p.

Rieger, M. and Rhein, L., 1997, Surfactants in cosmetics, New York, 635p.

Sadowski, Z. and Polowezyk, I., 2004, Agglomerate flotation of fine oxide particles, *Int. J. Miner. Process., 74:85-90.*

Schulz, J.C. and Warr, G.G., 2002, Adsorbed Layer Structure of cationic and Anionic surfactants on Mineral Oxide Surfaces, Langmuir, Australia, 6p.

Sedlak, A. and Janusz, W., 2008, Specific Adsorption of carbonate Ions at The Zinc Oxide/Electrolyte Solution Interface, Physicochemical Problems of Mineral Processing, 10p.

Stokes, R.J. and Evans, D.F., 1996, Fundamentals of Interfacial Engineering, Wiley-Vch, Canada, 605p.

Tulpar, A. And Ducker, W., 2004, Surfactant Adsorption at Solid-Aqueous Interfaces Containing Fixed Charges: Experiments Revealing The Role of Surface Charge Density and Surface Charge Regulation, J. Phys. Chem., 10p.

University of Malta, 2000, Determination of the Critical micelle Concentration (C.M.C.) of A Surfactant by conductivity Measurements, Department of Chemistry Physical Chemistry Practical IV, 8p.

Wang, W.L., Wang, Y.Y., Wan, C.C. and Lee, C.L., 2006, Self-assembly of Pd nanoparticles in dodecanol in situ generated from sodium dodecyl sulfate and its potential applications, *Colloids and Surfaces A: Physicochem. Eng. Aspects*, 275:11–16.

REFERENCES (continued)

Wöll, C., 2007, The chemistry and physics of zinc oxide surfaces, *Progress in Surface Science,* 82:55–120.

Zhuxi, F., 1995, ‘‘The wide gap semiconductor materials and their photo-electrical characteristic’’, http://www.ustc.edu.cn/1995,*(connection* date: 12.08.09).

RÉSUMÉ

Fırat Melih Gürsoy is born in Sivas/Zara in 1984. He has graduated from high school in 2000. He has graduated from Chemical Engineering Department of Engineering Faculty of Atatürk University in 2006.